Russian Chemical Reviews **70** (6) 471 – 490 (2001) © 2001 Russian Academy of Sciences and Turpion Ltd

DOI 10.1070/RC2001v070n06ABEH000657

Ultrafast nonradiative transitions between higher excited states in organic molecules

V L Ermolaev

Contents

I.	Introduction	471
II.	Single-photon excited fluorescence from higher excited S_n levels to the ground-state level	473
III.	Fluorescence due to transitions from higher excited S_n levels under conditions of stepwise excitation of molecules	476
IV.	Lifetimes of higher excited S_n states estimated from fluorescence quantum yields and absorption integrals	481
V.	Delayed fluorescence from higher excited S_n states due to triplet – triplet annihilation	481
VI.	Lifetimes of higher excited S_n states of molecules estimated from homogeneous broadening of absorption spectra	484
VII.	Lifetimes of higher excited S_n states estimated from picosecond and femtosecond spectroscopy data	486
VIII.	Ultrafast nonradiative transitions involving triplet states	487
IX.	Conclusion	488

Abstract. Ultrafast nonradiative transitions between electronic levels of aromatic and dye molecules, competing with fast photochemical reactions (*e.g.*, electron or proton transfer, photoisomerisation, *etc.*), are considered. The results of determination of the rate constants for nonradiative transitions between higher excited singlet and triplet states using different methods are summarised. The experimental data are interpreted in terms of the exchange-resonance theory of nonradiative transitions. The bibliography includes 189 references.

I. Introduction

In his lecture at the XIX Mendeleev Congress academician A L Buchachenko noted that the development of experimental techniques that use short laser pulses has widened the horizons of chemistry. Fresh ideas thus introduced into chemistry have been embodied into femtochemistry.[1] The subject of femtochemical studies is ultrafast reactions, such as proton or electron transfer in acid – base (donor – acceptor) pairs, *cis* – *trans*-isomerisation with detection of the *twist*-conformation, photogeneration and relaxation of electron-hole pairs in semiconductors, elementary stages in photosynthesis, molecular decomposition, *etc.*[2,3] Topicality of research into ultrafast processes is emphasised by the fact that the 1999 Nobel Prize in chemistry was awarded to A H Zewail, one of the originators of femtochemistry.

Single-photon excitation of a complex organic molecule to a higher excited singlet state (HESS) S_n ($n > 1$) is followed by transient relaxation processes. These processes, as well as transformations of excess electronic energy thus supplied to the molecule, are of considerable interest in studying the mechanisms of photochemical reactions in the vapour phase and in solutions. Most of the photochemical reactions of organic compounds in solutions are known to proceed involving the first excited singlet (S_1) and triplet (T_1) states. Both of them usually have rather long, on the molecular scale, lifetimes (from several nanoseconds for the S_1 states to hundreds of microseconds in liquids and tens of seconds in solid solutions for the T_1 states). However, the characteristic times of many fast photochemical reactions (electron and proton transfer, isomerisation, *etc.*) are much shorter. This suggests the involvement of other, upper excited states of the molecules (whose lifetimes are much shorter compared to those of the S_1 and T_1 states) in these reactions. Some of the fast reactions are considered in this review as examples. It should be noted that the possibility of estimating the HESS lifetimes has appeared only in the last decades. Nevertheless, a large body of experimental data obtained by direct and indirect methods has been accumulated to date. Therefore, it is of interest to analyse them, to assess their reliability and to consider possible mechanisms of excitation relaxation.

S I Vavilov was the first to obtain experimental data which allowed estimation of the rates of nonradiative transitions between the HESS of complex organic molecules (dyes) in solutions. He had shown experimentally[4,5] that the quantum yields of dye fluorescence in solutions are independent of the wavelength of exciting radiation. In other words, light emission (fluorescence) always occurs from the first excited (fluorescent) S_1 level irrespective of the level to which the molecule was excited after absorption of a light quantum (the Vavilov law).

Attempts to observe emission from the HESS of complex molecules under standard conditions have failed for long. This means that emission from these levels (with rate constants of the order of $10^7 - 10^8$ s^{-1}) is accompanied by a competing fast nonradiative process (with a rate constant of at least 10^{12} s^{-1}). This interpretation is also supported by the fact that the fluorescence spectrum of a complex molecule in solution is independent of the wavelength of exciting light.

After establishment of the triplet nature of the metastable phosphorescent state of aromatic molecules[6,7] the Vavilov law was supplemented by Kasha's rule,[8] according to which emission of light from complex molecules always occurs from the lowest excited level of a given spin multiplicity. The Vavilov law and Kasha's rule can be illustrated by a diagram of singlet (S_n) and triplet (T_n) vibronic energy levels of complex organic molecules (Fig. 1). Fulfilment of the Vavilov law and Kasha's rule means that the rate constants for nonradiative transitions (k_{nr}) from the S_n and T_n ($n \geqslant 2$) levels to the S_1 and T_1 levels, respectively, are

V L Ermolaev The State Unitary Enterprise 'All-Russian Scientific Centre, S I Vavilov State Optical Institute', Birzhevaya Liniya 12, 199034 St. Petersburg, Russian Federation. Fax (7-812) 328 37 20. Tel. (7-812) 328 46 08 (ext. 426). E-mail: ermol@soi.spb.su

Received 2 February 2001
Uspekhi Khimii **70** (6) 539 – 561 (2001); translated by A M Raevsky

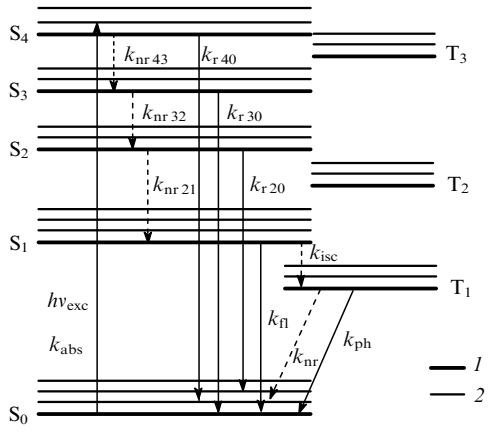


Figure 1. An energy level diagram illustrating transitions between vibronic levels of organic molecules.
Here and in Figs 2, 5–7 and 9 thick (*1*) and thin (*2*) lines denote electronic and vibronic energy levels, respectively. Notations of singlet energy levels: S_0 is the ground-state level and S_1, S_2, S_3 and S_4 are the first (fluorescent), second, third and fourth excited energy levels, respectively. Notations of triplet energy levels: T_1, T_2 and T_3 are the lowest (phosphorescent), second and third excited levels, respectively. Solid and dashed vertical lines respectively denote radiative and nonradiative transitions. Notations of rate constants: k_{r30} is the rate constant for the $S_3 \rightarrow S_0$ radiative transition (the radiative rate constant), $k_{r10} \equiv k_{fl}$ is the usual fluorescence rate constant, k_{nr32} is the rate constant for the $S_3 \rightarrow S_2$ nonradiative transition (internal conversion), k_{isc} is the rate constant for intersystem crossing (spin-forbidden $S_1 \rightarrow T_1$ nonradiative transition), k_{ph} is the phosphorescence rate constant, k_{nr} is the rate constant for nonradiative transition from the lowest triplet to the ground singlet state and k_{abs} is the absorption rate constant.

three for more orders of magnitude higher than the corresponding rate constants for radiative transitions (radiative rate constants, k_r) and intersystem crossing rate constants. However, this estimate says nothing about the rate constants for particular nonradiative transitions, *e.g.*, $S_n \rightarrow S_{n-1}$, $S_{n-1} \rightarrow S_{n-2}$, *etc*. However, knowledge of these rate constants is of interest for both research into fundamental problems of luminescence, photochemistry and photobiology and estimation of limiting energy characteristics of, *e.g.*, dye lasers and Q switches.

Recently, some experimental methods have been developed that allowed the obtaining of quantitative information on the rates of nonradiative transitions between higher excited energy levels of molecules. These are as follows:

1. Measurements of fluorescence spectra and yields from upper excited levels by direct single-quantum excitation of corresponding energy levels.

2. Measurements of $S_n \rightarrow S_0$ luminescence spectra and yields using a stepwise two-photon excitation technique, $S_0 + hv_1 \rightarrow S_1 + hv_2 \rightarrow S_n$ ($n > 1$).

3. Measurements of the fluorescence spectra from higher excited singlet levels populated *via* triplet–triplet annihilation.

4. HESS lifetime estimation from the results of (i) experiments on 'hole burning' in absorption spectra at low temperatures, (ii) linewidth measurements in fluorescence excitation spectra in supersonic jets or (iii) bandwidth measurements in structured emission spectra from higher excited levels.

5. Direct HESS lifetime measurements using picosecond or femtosecond spectroscopy.

6. Estimation of the rates of ultrafast nonradiative transitions involving triplet states.

Before presenting the results of particular experimental studies on the rates of nonradiative transitions we will briefly outline elements of modern quantum-mechanical theories of nonradiative transitions in complex organic molecules. According to formal theory of nonradiative transitions,[9–11] excitation of a molecule leads to its transition to a non-stationary excited state. Owing to short duration of the excitation pulse and high density of final vibronic states inherent in polyatomic molecules, nonradiative deactivation of the initial non-stationary state occurs exponentially. The rate constant for such a process, k_{nr}, is calculated using first-order, time-dependent perturbation theory. This process corresponds to the 'statistical limit' case.[12]

If the adiabatic approximation holds, the wave function of the system, $\Psi_{ma}(\mathbf{r}, \mathbf{Q})$, can be written as the product of electron wave function, $\varphi_{ma}(\mathbf{r}, \mathbf{Q})$, and vibrational wave function, $\chi_a(\mathbf{Q})$,

$$\Psi_{ma}(\mathbf{r}, \mathbf{Q}) = \varphi_m(\mathbf{r}, \mathbf{Q})\chi_a(\mathbf{Q}),$$

where $\mathbf{r}(r_1, r_2, r_3,...)$ are the electron coordinates, $\mathbf{Q}(Q_1, Q_2, Q_3,...)$ are the coordinates of atomic nuclei and the indices m and a denote the energy level and vibrational state, respectively.

Usually, the operator of nonadiabaticity, $V_{ma,nb}$ (m and n denote the energy levels and a and b denote the corresponding vibrational states), is considered as a perturbation inducing the nonradiative transition. Approximate expression for the matrix element of transition between the excited electronic state n and the state m with a lower energy has the form:

$$V_{ma,nb} \approx$$
$$\approx -\sum_i \frac{h^2}{M_i} \int \chi_{ma}(\mathbf{Q}) \left\langle \varphi_m(\mathbf{r}, \mathbf{Q}) \left| \frac{\partial}{\partial Q_1} \right| \varphi_n(\mathbf{r}, \mathbf{Q}) \right\rangle \frac{\partial}{\partial Q_1} \chi_{nb}(\mathbf{Q}) \mathrm{d}\mathbf{Q} +$$
$$+ \frac{1}{2} \sum_i \frac{h^2}{M_i} \int \chi_{ma}(\mathbf{Q}) \left\langle \varphi_m(\mathbf{r}, \mathbf{Q}) \left| \frac{\partial^2}{\partial Q_1^2} \right| \varphi_n(\mathbf{r}, \mathbf{Q}) \right\rangle \chi_{nb}(\mathbf{Q}) \mathrm{d}\mathbf{Q},$$

where M_i is the mass of the nucleus of ith atom. Neglecting the term containing the second derivatives of electron wave functions and simplifying this expression,[13] we get

$$V_{ma,nb} \approx \left\langle \varphi_m(\mathbf{r}, \mathbf{Q}) \left| \frac{\partial}{\partial Q_i} \right| \varphi_n(\mathbf{r}, \mathbf{Q}) \right\rangle = \frac{\langle \varphi_m(\mathbf{r}, \mathbf{Q}) | \partial U / \partial Q_i | \varphi_n(\mathbf{r}, \mathbf{Q}) \rangle}{E_m(\mathbf{r}, \mathbf{Q}) - E_n(\mathbf{r}, \mathbf{Q})},$$

where $U(\mathbf{r},\mathbf{Q})$ is the Coulomb energy of the interaction between electrons and nuclei and $E(\mathbf{r},\mathbf{Q})$ is the adiabatic potential for the excited state.

The total rate of a nonradiative transition between the states n and m can be written as the sum of partial transition probabilities

$$k_{r\,nm} = \frac{2\pi}{h} \sum_{a,b} |V_{ma,nb}|^2 p(nb) \delta(E_{ma} - E_{nb}).$$

Here, $p(nb)$ is the population of the initial vibronic state, δ is the Dirac delta function and E_{ma} and E_{nb} are the energies of the vibronic states ma and nb, respectively.

The aforesaid represents a framework of the general theory of nonradiative transitions. In the text below, we will consider the exchange-resonance theory of nonradiative transitions in ions and complex molecules developed by Sveshnikova, the author of this review and Bodunov.[14–16] According to this theory, all vibrations of a molecule under study are divided into two types, namely, promoting-accepting vibrations and accepting ones.

The first type of vibrations comprises high-frequency, strongly anharmonic vibrations responsible for the vibrational absorption spectrum of the molecule in both fundamental and overtone regions. These vibrations are usually almost inactive in vibronic molecular spectra since corresponding Franck–Condon integrals are close to zero.

The second type of vibrations comprises those responsible for the vibronic spectrum of the molecule due to nonzero Franck–Condon integrals. Often, these vibrations appear to be totally symmetric and are therefore inactive in the vibrational absorption spectrum of the molecule. For instance, the totally symmetric vibrations of aromatic molecules associated with changes in the C–C distances belong to accepting vibrations.

Bodunov[15] used the operator of nonadiabaticity as a perturbation inducing the nonradiative transition. He divided molecular

vibrations into two above-mentioned types and showed that the expression for the rate constant for the nonradiative transition between two electronic levels, k_{nr}, can be written using the overlap integral of the normalised vibronic emission spectrum of a molecule due to transition between the corresponding levels, $f(E)$, and the vibrational absorption spectrum of the same molecule, $\sigma(E)$

$$k_{nr} \approx \left|\overline{\langle\varphi_m|\frac{\partial U}{\partial Q_k}|\varphi_n\rangle}\right|^2 \int f(E)\sigma(E)E^{-(s+1)}\mathrm{d}E.$$

Here, the horizontal line denotes averaging over the first type of vibrations; $s = 3$ for dipole and $s = 5$ for quadrupole radiation. This formula is similar to the Förster–Dexter formulae for the nonradiative energy transfer between energy donor and acceptor, except that the transfer occurs intramolecularly to decrease the electron energy and to increase the vibrational energy. Validity of the exchange-resonance theory of nonradiative transitions was experimentally proved taking lanthanide ions in solutions,[14,17] transition-metal complexes[17,18] and (with some limitations) complex aromatic molecules[17–19] as examples. It should be noted that this theory was developed assuming a weak coupling between the energy levels involved in the transition, though this is not necessarily true in the case of HESS.

In this review, we will analyse the results of experimental studies from the standpoint of the exchange-resonance theory of nonradiative transitions, since this theory predicts that k_{nr} is proportional to k_r. Unfortunately, the rate constants for radiative transitions between higher excited singlet states are unknown for most of the molecules studied; nevertheless, in some instances such correlations can be found.

Recently, a number of reviews concerning fast photophysical and photochemical processes in complex organic molecules have been published (see, *e.g.*, excellent reviews[20,21]). However, the authors of these studies placed the emphasis on the vibrational energy redistribution after excitation of the molecules, whereas the problem of electronic relaxation was only briefly outlined. On the other hand, a large body of information on electronic relaxation reported in numerous studies allows some generalisation of the results obtained.

II. Single-photon excited fluorescence from higher excited S_n levels to the ground-state level

Beer and Longuet-Higgins[22] were the first who reported a strongly supported example of violation of the Vaviov law and Kasha's rule. They studied fluorescence of an azulene solution under conditions of single-quantum excitation and provided convincing proofs of the fact that the fluorescence observed after excitation of the solution into the second or shorter-wavelength absorption bands is due to transition from the second excited to the ground-state level ($S_2 \rightarrow S_0$). Azulene fluorescence was observed in the near UV spectral region (at about 28 000 cm^{-1}), though the long-wavelength absorption band of this compound lies near 14 000 cm^{-1}. These experimental observations were confirmed in more recent studies of azulene and a large number of its derivatives.[23–25] The quantum yields of $S_2 \rightarrow S_0$ fluorescence of a number of azulene derivatives were found to be as high as several percent while the S_2 state lifetimes were as long as 1.4 ns. The results obtained in these studies were briefly outlined in a monograph.[26]

Much weaker was the $S_2 \rightarrow S_1$ fluorescence of azulene observed in the region from 14 000 to 9500 cm^{-1} (710–1050 nm).[27–30] Thorough measurements allowed[31] the determination of the quantum yield ratio of the $S_2 \rightarrow S_0$ and $S_2 \rightarrow S_1$ fluorescence ($q_{fl\,20}$ and $q_{fl\,21}$, respectively)

$$\frac{q_{fl\,20}}{q_{fl\,21}} = 450 \pm 100.$$

This value characterises the ratio of the rate constants for radiative transitions from the S_2 level to the ground-state and first excited levels. From the standpoint of the exchange-resonance theory of nonradiative transitions[14] the low probability of $S_2 \rightarrow S_1$ internal conversion is due to not only the wide energy gap between these levels and minor changes in the molecular configuration in the S_1 state compared to those for the molecular configuration in the S_2 state, but also forbiddenness of the radiative transition between these levels.

Hirata and Lim[32] studied fluorescence of azulene and perdeuterated azulene vapours and, in particular, its dependence on the excess vibrational energy in the S_2 state. They suggested that a direct internal conversion from the second excited singlet state to the ground state can occur in the azulene molecule bypassing the S_1 state. Unfortunately, this assumption was not strengthened by convincing proofs, so that the arguments adduced by the authors had little force.

$S_2 \leftarrow S_0$-Fluorescence excitation spectra of azulene cooled in a supersonic jet have been studied.[33] It was found that the fluorescence excitation spectrum of the $S_2 \leftarrow S_0$ transition exhibits a fine vibrational structure. The fluorescence excitation spectra for transitions from the ground-state level to the S_3 and S_4 levels were found to be substantially broadened due to fast conversion from these levels to the S_2 state.

Direct measurements of fluorescence decay times from the S_2 state of 2-haloazulene and 1,3-dihaloazulene molecules in solution have been carried out.[34] It was shown that intersystem crossing to the triplet manifold with the rate constant $k_{isc}(S_2 \rightsquigarrow T_n)$ can occur in the molecules of compounds studied in addition to the $S_2 \rightsquigarrow S_1$ internal conversion and $S_2 \rightarrow S_0$ and $S_2 \rightarrow S_1$ transitions.

Table 1 lists the fluorescence quantum yields, energy level positions [$E(S_2)$], energy gaps (ΔE), rate constants for radiative and nonradiative transitions between different energy levels as well as the second excited singlet state lifetimes, $\tau(S_2)$, for azulene and a number of its derivatives.[31–51] For comparison, mention may be made that the $S_1 \rightarrow S_0$ fluorescence of azulene in solution ($\sim$14 000 cm^{-1}) is characterised by very low quantum yield ($\sim 10^{-4}$–10^{-6}) (see Refs 24 and 35) and a decay time, $\tau(S_1)$, estimated at 1.9 (see Ref. 36) or 1 ps (see Ref. 37).

The dynamics of isolated azulene molecules in the S_1 state has been studied in detail by femtosecond-resolved mass spectrometry in molecular beams.[38] The dephasing time of azulene was found to be shorter than 100 fs. With an excess vibrational energy of $\sim$2000 cm^{-1}, the $S_1 \rightarrow S_0$ internal conversion time in azulene vapours was estimated at 900±100 fs. It was concluded that, despite the wide energy gap ($\sim$14 000 cm^{-1}), such a high internal conversion rate can be rationalised by considering the conical intersection of the potential energy surfaces (PES) of the S_1 and S_0 states near the PES minimum of the S_1 state, as was suggested earlier.[22,39]

Luminescence studies[40] of azulene derivatives allowed the determination of the order in which light emission appears. At low temperatures, an increase in the energy of the S_1 level and narrowing of the $\Delta E(S_2-S_1)$ gap lead to the appearance of the $S_1 \rightarrow S_0$ fluorescence. At room temperature, the $S_2 \rightarrow S_0$ fluorescence remains the dominant process. At higher temperatures, the usual $S_1 \rightarrow S_0$ fluorescence prevails. A feature of azulene derivatives is the low-temperature $T_1 \rightarrow S_0$ phosphorescence.

Interesting results were obtained in studies of the fluorescence of 1,3,5,7-tetra-*tert*-butylindacene (TTBI), a representative of nonalternant antiaromatic hydrocarbons.[41] Similarly to azulene, TTBI has a low intensity transition in the near IR region [$E(S_1)$ = 9300 cm^{-1}] and has an intense, allowed transition in the visible spectral region [$E(S_2)$ = 18 300 cm^{-1}]. The authors of this study[41] succeeded in observing the $S_2 \rightarrow S_0$ fluorescence of a TTBI solution in cyclohexane (see Table 1). A salient feature of this compound is violation of the cascade character of internal conversion, so that the $S_2 \rightsquigarrow S_0$ nonradiative transition appears to be more probable than the $S_2 \rightsquigarrow S_1$ transition. In accordance with the proposed exchange-resonance mechanism of nonradiative transitions,[15] this violation can be suggested to be due to substantial increase in the probability of the $S_2 \rightarrow S_0$ radiative

Table 1. Characteristics of transitions from the second singlet level for a number of organic molecules.

Compound	Solvent	$E(S_2)$ /cm^{-1}	$\Delta E(S_2-S_1)$ /cm^{-1}	$q_{fl\,20}$	$k_{r\,20}$ /s^{-1}	$\tau(S_2)$ /ps	$10^{-8}\,k_{nr\,21}$ /s^{-1}	Ref.
Azulene	cyclohexane	28 300	14 000	3.1×10^{-2}	2.2×10^{7}	1400	6.9	35
	isopentane (at 190 K)	28 300	14 000	6.8×10^{-5} (see [a])	4.0×10^{4} (see [b])	1400	5.9	31
1,3-Dichloroazulene	cyclohexane	27 000	14 300	5.8×10^{-2}	3.6×10^{7}	830	6.934	34
1,3-Dibromoazulene	ethanol	–	12 400	4.4×10^{-2}	5.5×10^{7}	310	–	34
1,3,5,7-Tetra-*tert*-butylindacene	cyclohexane	18 300	9100	9×10^{-5}	10^{8}	2.5	4×10^{3} (see [c])	41
Xanthione	fluorinated hydrocarbons	24 000	7970	1.4×10^{-3}	8×10^{6}	175	5.7×10	51
	trimethylpentane	23 400	7500	5×10^{-4}	1×10^{7}	45	2.1×10^{5}	49
2,2,3,3-Tetramethyl-indanethione	fluorinated hydrocarbons	26 800	11 000	1.4×10^{-1}	1.6×10^{8}	880	9.7	51

Note. Measurements were mostly carried out by direct single-quantum excitation at room temperature.
[a] The $q_{fl\,21}$ value, [b] the $k_{r\,21}$ value, [c] the $k_{nr\,20}$ value.

transition compared to that of the $S_2 \rightarrow S_1$ transition and to the larger value of the Franck–Condon factor for the former transition. According to quantum-mechanical calculations,[41] the geometric parameters of the TTBI molecule in the S_2 and S_1 states are close, but they differ appreciably from those for the S_0 state.

Fluorescent properties of solutions of another representative of antiaromatic compounds, 1,3,5-tri-*tert*-butylpentalene, have been studied theoretically and experimentally.[42] Emission observed in the region near 27 000 cm^{-1} with a quantum yield of 2×10^{-3} after excitation by light with $\lambda = 313$ nm was assigned to the $S_3 \rightarrow S_0$ transition. The interpretation of the results obtained in this study appeared to be the subject of a discussion.[4,44] The role of conical intersection of the PES of the S_1 and S_0 states in quenching of usual fluorescence was pointed out.[44]

A study of fluorescence from the second excited singlet level of [18]-annulene (18A), a representative of alternant hydrocarbons, and its monofluoro derivative (F18A) in 3-methylpentane matrix at 4 K has been reported.[45] Symmetric (D_{6h}) molecular skeleton of 18A comprises 18 carbon atoms while the S_1 and S_2 states of the molecule are in the regions of 12 500 and 21 400 cm^{-1}, respectively. Both 18A and F18A were found to be $S_2 \rightarrow S_0$ fluorescent with rather high yields, the latter being also $S_1 \rightarrow S_0$ fluorescent (in this case, the fluorescence yield was 100 times lower). Nickel and Hertzberg[46] studied fluorescence of biphenylene (an antiaromatic hydrocarbon) in 3-methylpentane solution at 130 K. They found that the fluorescence yield from the second excited level is more than two orders of magnitude lower than that of the $S_1 \rightarrow S_0$ fluorescence, namely, $q_{fl}(S_1 \rightarrow S_0) = 2.3\times10^{-4}$.

Thioketones represent another class of compounds characterised by rather high fluorescence yields for transitions of their molecules from the second excited singlet state.[47–50] Huber and Mahaney were the first who reported the emission from the S_2 level of aromatic thioketone molecules taking xanthione as an example.[47] Shortly, their paper was followed by a series of related studies carried out using a large number of alkyarylthioketones.[48–50] For thioketone molecules, the orbital forbidden $S_1(n,\pi^*) \leftarrow S_0$ transition is near 15 000 cm^{-1} (the molar extinction coefficient at the absorption band maximum, ε_{max}, is 20 mol^{-1} litre cm^{-1}), while the allowed $S_2(\pi,\pi^*) \leftarrow S_0$ transition is near 23 500 cm^{-1} ($\varepsilon_{max} = 16\,000$ mol^{-1} litre cm^{-1}).[49,51]

The $S_2 \rightarrow S_0$ fluorescence bands are observed in the violet spectral region ($\sim$22 500 cm^{-1}) while those of the long-wavelength $S_1 \leftarrow S_0$ transition are observed in the near IR spectral region ($\sim$15 000 cm^{-1}). It should also be noted that no $S_1 \rightarrow S_0$ fluorescence was found. On the other hand, $T_1 \rightarrow S_0$ phosphorescence is observed even at room temperature, with a quantum yield (in frozen solution) can be as high as 10%.

Fluorescence from the second excited state of xanthione and related molecules is strongly quenched upon addition of saturated and aromatic hydrocarbons, which is indicative of a photochemical reaction between the thioketones and hydrocarbons.[50–54] The highest $S_2 \rightarrow S_0$ fluorescence yields were obtained in solutions of perfluoroalkanes (*e.g.*, $q_{fl\,20} = 0.014$ for xanthione at room temperature, see Table 1). The dipole $S_2 \rightarrow S_1$ radiative transition in the xanthione molecule is forbidden.[49] This substantially decreases the probabilities of nonradiative transitions in accordance with the proposed exchange-resonance mechanism of these transitions.[15]

A solution of 4-*H*-1-benzopyran-4-thione (BPT) in perfluoro-1,3-dimethylcyclohexane has been studied in detail.[55–57] It was shown that the phosphorescence quantum yield is independent of the frequency of exciting light up to 36 300 cm^{-1} (the $S_0 \rightarrow S_4$ transition). This fact contradicts the conclusion drawn previously[58,59] that the phosphorescence yield decreases by 30% upon excitation into the $S_0 \rightarrow S_1$ band as compared to direct excitation to the T_1 state. On the other hand, a 25% decrease in the $S_2 \rightarrow S_0$ fluorescence yield under excitation into the $S_0 \rightarrow S_4$ band was found. This was associated with changes in the rate of internal conversion from the S_2 state;[57] is it also implied that excitation to upper states leads to an increase in the vibrational energy of the molecule. Intersystem crossing from the HESS to the triplet manifold (namely, to higher excited triplet levels) due to the strong spin-orbit coupling, followed by fast internal conversion to the T_1 state also seems not to be improbable in thioketones.

Maciejewski *et al.*[60] proposed a method for determination of quantum yields of intramolecular nonradiative transitions, $q_{nr}(S_m \rightarrow S_{m-i})$ ($i = 1, 2, \ldots, m$), between different energy levels of complex organic molecules. The method was evaluated taking three aromatic thioketones dissolved in a perfluorinated hydrocarbon and directly excited to the S_3 state as examples. To determine the $q_{nr}(S_m \rightarrow S_{m-i})$ values, the relative fluorescence quantum yields $q_r(S_{m-1})$, $q_r(S_{m-2})$, ... $q_r(S_1)$ from all lower lying energy levels should be known. The authors of this study used the phosphorescence yield of thioketones, $q_r(T_1)$, instead of the usual fluorescence yield, $q_r(S_1)$, assuming that the T_1 state is populated exclusively *via* the S_1 state and thioketones exhibit no S_1 fluorescence. (The latter statement is incorrect since it is known[55,57] that for BPT the S_1 fluorescence intensity is $\sim$0.01 of the phosphorescence intensity at room temperature.) The relative quantum yields of nonradiative transitions between different excited singlet levels can also be estimated by comparing the absorption and fluorescence excitation spectra from different lower-lying energy levels. The internal conversion and emission quantum yields (q_{nr} and q_r, respectively) for the three thioketones are listed in Table 2.

The starting point of the study[60] was to rationalise marked violations of the cascade mechanism of internal conversion observed even for molecules with rather wide energy gaps (this

Table 2. Characteristics of nonradiative and radiative transitions in thioketones dissolved in perfluoro-1,3-dimethylcyclohexane, obtained at room temperature.[60]

Transition characteristics	Xanthione-1,3,4,5,6,8-d_6	Xanthione-h_8	4*H*-1-Benzopyran-4-thione
$q_{nr}(S_4 \rightsquigarrow S_2)$	–	–	(0.74)
$q_{nr}(S_3 \rightsquigarrow S_2)$	0.90	0.72	0.74 (0.82)
$q_{nr}(S_3 \rightsquigarrow S_1)$	0.0	0.04 (?)	0.11 ($\sim$0.0)
$q_{nr}(S_3 \rightsquigarrow S_0)$	0.10 (?)	0.24 (?)	0.15 ($\sim$0.0)
$q_{nr}(S_2 \rightsquigarrow S_1)$	0.96	0.85	0.88 (1.0)
$q_{nr}(S_2 \rightsquigarrow S_0)$	0.0	0.14 (?)	0.10 ($\sim$0.0)
$q_r(S_2 \rightsquigarrow S_0)$	0.042	0.014	0.023
$q_r(T_1 \rightsquigarrow S_0)$	0.078	0.038	0.076
$q_r(S_1 \rightsquigarrow S_0)$	0.0	0.0	0.0 (0.01)
$\tau(S_2)$ /ps	606	178	210
$E(S_1)$ /cm^{-1}	16 000	16 000	16 800
$\Delta E(S_2-S_1)$ /cm^{-1}	8000	7900	8600
$\Delta E(S_3-S_2)$ /cm^{-1}	4900	5000	4800
$\Delta E(S_3-S_1)$ /cm^{-1}	12 900	12 900	13 400

Note. The data taken from Ref. 57 are given in parentheses.

particularly refers to quantum yields of the $S_3 \rightsquigarrow S_0$ and $S_2 \rightsquigarrow S_0$ nonradiative transitions, see Table 2). The authors cited suggested that these violations can be accounted for either by large differences between the electronic matrix elements appearing in the expression for the rate constant of nonradiative transition or by conical intersection of the PES when moving over the hypersurface of the S_3 state towards a distorted local minimum. In interpretation proposed in the study,[16] the above-mentioned matrix elements represent the rate constants for radiative transitions between corresponding energy levels. Conical intersection of the PES provides a direct transition to the ground state.

Difficulties in measuring q_{nr} should be pointed out. First, this is a strong overlap of the bands corresponding to population of different HESS in the absorption spectrum, especially if the intensities of neighbouring bands differ substantially, as is the case of the $S_3 \rightsquigarrow S_0$ and $S_2 \rightsquigarrow S_0$ transitions in thioketones. Because of this, information on violation of cascade mechanism of nonradiative transitions between excited levels in particular molecules including thioketones should be considered very carefully. For instance, Nickel[61] thoroughly studied nonradiative transitions in BPT and came to conclusion that there is no good reason to assume direct internal conversion from the S_2 and S_3 states of thioketone molecules to the ground state.† Fast appearance of an impurity (a photochemical reaction product) in the thioketone solution has also been reported.[56]

The method proposed by Maciejewski *et al.*[60] allows the obtaining of complete information on the nonradiative transitions between all energy levels only if direct single-quantum excitation of a HESS will give rise to fluorescence from all lower-lying levels. However, this is possible (and only for the S_2 state!) for a limited number of molecules (thioketones, several porphyrins, *etc.*). If direct single-quantum excitation gives rise only to S_1 fluorescence, one can only point to deviations from the Vavilov law and Kasha's rule which were repeatedly checked using many molecules.

Bright $S_2(\pi,\pi^*) \rightarrow S_0$ fluorescence of 1,8-(1′,8′)-naphthalylnaphthalene solutions, characterised by $q_{fl} = 0.18$ and $t = 3$ ns was observed,[62] despite the narrow gap between S_2 and S_1 levels [$\Delta E(S_2-S_1) = 5000$ cm^{-1}]. However, such a high quantum yield of fluorescence due to transition from the S_2 level in combination with the narrow energy gap seems to be unrealistic. Presumably, in this case there was a contribution of impurity or product of a photochemical reaction. Similarly to thioketones and azulene, no $S_1(n,\pi^*) \rightarrow S_0$ usual fluorescence was observed, only phosphorescence was found in this case.

† Private communication.

Direct single-quantum excitation of porphin derivatives also gives rise to the $S_2 \rightarrow S_0$ (or $S_3 \rightarrow S_0$) fluorescence. This fluorescence ($\sim$23 000 cm^{-1}) was first studied by Gouterman *et al.*[63] The fluorescence spectrum was found to be a mirror image of intense Soret absorption band. More detailed studies of this fluorescence have shown[64,65] that the highest quantum yield ($q_{fl\,20} = 1.2 \times 10^{-3}$) is observed for Zn-tetrabenzoporphyrin solutions. For metal-free tetrabenzoporphyrin, the absolute quantum yield of 'blue' fluorescence is nearly an order of magnitude lower (1.8×10^{-4}). It was also found that tetrabenzoporphyrin complexes with metals with partly filled *d*-shell exhibit no 'blue' fluorescence detectable under conditions of single-quantum excitation.

In a study[66] of Co(II) and Ni(II) complexes with crown ethers and phthalocyanine derivatives it was shown that the $S_2 \rightarrow S_1$ internal conversion time is shorter than 500 fs. Effect of complexation of *meso*-tetraphenylporphyrins (TPP) with trivalent Y, Lu and Th on the 'blue' fluorescence has been studied.[67] All the complexes under study, *viz.*, YTPP(acac), LuTPP(acac) and ThTPP(acac), exhibit fluorescence from the S_2 level with nearly equal quantum yields (0.001). In contrast to this, the quantum yield of usual fluorescence of these complexes decreases substantially in the above-mentioned order, which indicates that intersystem crossing has no effect on quenching of the S_2 level of porphyrins. No fluorescence from the second singlet level was found for free base TPP.[67,68] In spite of nearly equal energy gaps $\Delta E(S_2-S_1)$ for metal complexes with octaethylporphyrins (OEP) and TPP, such OEP as H_2OEP, AlClOEP and ZnOEP exhibit no $S_2 \rightarrow S_0$ fluorescence.[68] $S_2 \rightarrow S_0$-Fluorescence of tetra-*para*-tolylporphyrin complexes with Sm(III), Eu(III), Gd(III), Tb(III), Yb(III) and Lu(III) in ethanol has been studied.[69] Weak quenching (by factors of $\sim$1.5 to 3.0) of fluorescence of paramagnetic complexes with Gd(III), Sm(III) and Tb(III) as well as strong quenching of fluorescence for the complexes with Eu(III) and Yb(III) was explained by the appearance of charge-transfer states lying between the S_1 and S_2 levels on the energy scale. [Among lanthanide ions, Eu(III) and Yb(III) are known to possess the highest electron affinities.]

Due to the short lifetime of the S_2 state, 'blue' fluorescence of porphyrins is strongly polarised even in solutions of low viscosity (in contrast to usual $S_1 \rightarrow S_0$ fluorescence of organic compounds).[60] This feature was used[70] to separate out the $S_2 \rightarrow S_0$ fluorescence. Frequency modulation was performed using polarisers while signal measurements were carried out with an amplifier with synchronous detection. This experimental procedure allows one to separate out the desired fluorescence against the background of the impurity usual fluorescence, since the impurities emit natural light and their signal is not modulated. The quantum yield of S_2 fluorescence of Zn-ethioporphyrin under conditions of single-quantum excitation was 7.5×10^{-5}. An up-conversion study of the S_2 fluorescence decay and S_1 fluorescence rise of Zn(TPP) complexes in ethanol has been reported.[71] It was shown that the decay of the S_2 fluorescence at 430 nm and the rise of the S_1 fluorescence near 600 nm are characterised by the same time constant of 2.3 ps. A more complex picture is observed for the spectral region between these bands, which indicates a contribution of 'hot' luminescence.

$S_2 \rightarrow S_0$-Fluorescence studies of dye molecules under conditions of single-quantum excitation have been carried out taking Brilliant Green[72] and Malachite Green[73,74] dyes as examples.

Lipsky *et al.*[75–77] studied single-quantum induced fluorescence of aromatic molecules from the second and upper levels. Alkylbenzenes were excited with a Hg resonance line at $\lambda = 184.9$ nm (the vacuum UV spectral region). Very weak $S_2 \rightarrow S_0$ (or $S_3 \rightarrow S_0$) fluorescence bands appeared on the short-wavelength wing of the usual fluorescence spectra. To single them out, quenchers of usual fluorescence (CCl_4, CCl_3H, cyclo-C_7F_{14}) were added to the solutions. In contrast to usual fluorescence,

Table 3. Characteristics of nonradiative transitions from the second (or upper) singlet levels in a number of organic molecules.

Compound	Solvent	$E(S_2)$ /cm^{-1}	$\Delta E(S_2-S_1)$ /cm^{-1}	$q_{fl\,20}$	$k_{r\,20}$ /s^{-1}	$\tau(S_2)$ /ps	$k_{nr\,21}$ /s^{-1}	Ref.
Zn-Tetrabenzoporphyrin	–	23 300	7400	1.2×10^{-3}	5.2×10^{8}	3	3.3×10^{11}	65
		–	–	(1.6×10^{-3})	–	–	–	63
Zn-Ethioporphyrin	DMF	24 450	7200	7.5×10^{-5}	–	–	–	70
Tetrabenzoporphyrin	"	–	–	1.8×10^{-4}	–	0.4	2.5×10^{12}	70
Brilliant Green	ethanol, 77 K	21 800	6300	1.0×10^{-4}	5×10^{7}	2	5×10^{11}	72
p-Xylene	isooctane	41 000	6600	2.9×10^{-5}	2.9×10^{8}	0.1	1.0×10^{13}	75
	"	–	(34 400)	(1.3×10^{-5})	–	–	(1.5×10^{14})	77
	"	48 800 (see [a])	7800 (see [b])	1.2×10^{-5}	3.0×10^{9} (see [c])	0.004	2.5×10^{14}	75
		–	–	(5×10^{-6})	–	–	–	77
Naphthalene	"	44 050 (see [a])	–	2.2×10^{-5}	–	–	(8×10^{13})	76
	"	–	–	(2×10^{-5})	–	–	–	77
Pyrene	"	36 000 (see [a])	7000	5×10^{-6}	–	–	–	76

Note. Measurements were carried out using direct single-quantum excitation technique at room temperature. The values obtained from measurements in the vapour phase are given in parentheses. [a] The $E(S_3)$ value, [b] the $E(S_3-S_2)$ value, [c] the $k_{r\,30}$ value.

almost no quenching of the S_2 and S_3 fluorescence occurs due to the short lifetimes of these states. Presumably, impurity emission that precludes the observation of fluorescence from HESS of the molecules under study is also quenched simultaneously. Selected characteristics of nonradiative transitions in these molecules are listed in Table 3. High rates of internal conversion and small differences between them in solutions and as vapours, indicative of intramolecular process, are noteworthy.

Carotenoids play an important role in many processes occurring in living organisms. In particular, they serve as pigment protectors in cells of green plants and purple bacteria against their destruction by singlet oxygen. A systematic study of fluorescence of β-carotenes and their analogues, linear polyenes, has been carried out.[78] It was found that the energy gap $\Delta E(S_1-S_0)$ becomes narrower and the yield of usual fluorescence decreases as the polyene chain length increases. The fluorescence yield decreases from 7×10^{-3} for the polyene with five conjugated bonds down to 4×10^{-6} for β-carotene (solutions in hexane at room temperature). Among the compounds under study, the longest molecular chains were those of decapreno-β-carotene and dodecapreno-β-carotene with 15 and 19 double bonds, respectively. These compounds exhibited only S_2 fluorescence with the quantum yield $q_{fl\,20}\approx5\times10^{-5}$. The S_2 state lifetime, $\tau(S_2)$, estimated from q_{fl20} was $\sim$100 fs. Therefore, despite the decrease in the usual fluorescence yield with lengthening of the molecular chain, fluorescence from the second excited level of these molecules remains nearly constant.

Weak $S_2\rightarrow S_0$ fluorescence was observed in an anthracene crystal directly excited by a resonance Hg line at $\lambda=254$ nm.[79] The ratio of fluorescence yields from the S_2 and S_1 states was estimated at $\sim5\times10^{-6}$ and $\tau(S_2)$ was roughly estimated at $\approx10^{-13}$ s.

However, measurements of fluorescence spectra and quantum yields of fluorescence due to transitions from the second and upper excited singlet states under conditions of direct single-quantum excitation are impossible for most of fluorescent complex organic compounds. This is due to the low fluorescence quantum yields, superimposition of impurity luminescence in solvents and in insufficiently purified substances under study and to the Rayleigh and Raman scattering.

In conclusion, mention may be made of an interesting example of fluorescence from a triplet rather than singlet higher excited state.[80] Irradiation of 9,10-dibromoanthracene and 9-bromoanthracene solutions in undegassed hexane by a high-power Xe lamp resulted in weak fluorescence near 840 nm for the former and near 865 nm for the latter compound. This phenomenon was suggested to be due to the $T_2\rightarrow T_1$ radiative transition. Fluorescence was excited in the regions of conventional absorption spectra of these compounds. The T_2 levels were populated *via* $S_1\rightarrow T_2$ intersystem crossing. The T_2 levels of the molecules under study are near the corresponding S_1 levels on the energy scale and the energy gaps, $\Delta(T_2-T_1)$, are $\simeq12\,000$ cm^{-1}. The $T_2\rightarrow T_1$ fluorescence quantum yield was estimated at 8×10^{-7} and the T_2 state lifetime, $\tau(T_2)$, was estimated at $\simeq10^{-11}$ s.[80]

III. Fluorescence due to transitions from higher excited S_n levels under conditions of stepwise excitation of molecules

The appearance of pulsed laser excitation sources allowed studies of ultrafast relaxation processes from HESS using the stepwise excitation technique. Essentially, the method is as follows. Excitation of a molecule by the first quantum leads to population of the first (fluorescent) excited singlet state S_1. Being in the thermalised S_1 state, the molecule absorbs the second quantum, thus populating an upper excited singlet state (Fig. 2)

$$S_0+h\nu_1\rightarrow S_1+h\nu_2\rightarrow S_n\ (n\geqslant2).$$

This excitation technique allows easy observation of fluorescence spectra corresponding to $S_n\rightarrow S_0$ transitions ($n\geqslant2$) with quantum yields of the order of $10^{-6}-10^{-7}$. It appears to be

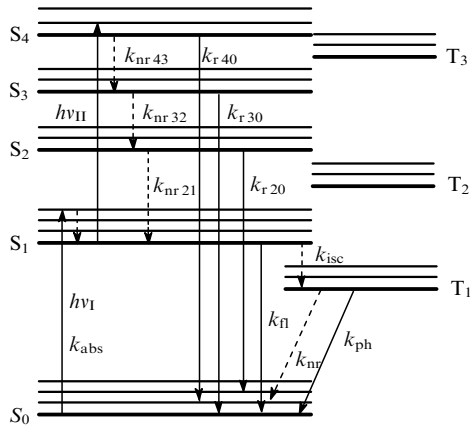


Figure 2. An energy level diagram illustrating nonradiative transitions between higher excited singlet states under conditions of two-quantum stepwise excitation and fluorescence due to transitions from the HESS to the ground state of the molecule;
$h\nu_I$ and $h\nu_{II}$ are the first and second excitation quanta, respectively.

particularly convenient when using tunable lasers generating nanosecond pulses and operating at repetition rates from 5 to 50 Hz. The method has the advantage that stepwise excitation has no effect on the fluorescent impurity molecules in the compound under study and in the solvent, whose absorption spectra are observed in the region of $S_n \leftarrow S_0$ ($n \geqslant 2$) transitions. In addition, the spectrum under study is not overlapped with the Raman spectrum since the latter is shifted up to 3000 cm^{-1} with respect to the former. To simplify the interpretation of the results obtained, nanosecond pulses were used with moderate radiation flux levels. (In this case, the use of picosecond and femtosecond laser pulses is less appropriate since it is accompanied by an increase in the contribution of two-photon excitation which affects also the impurity molecules). The best combination of molecular properties for performing stepwise excitation studies includes sufficiently high fluorescence yields, S_1 state lifetimes of the order of several nanoseconds and rather large absorption cross-sections for the $S_n \leftarrow S_1$ transitions.[81]

The first studies on fluorescence spectra corresponding to transitions from higher excited states to the ground state obtained by stepwise excitation technique date back to the late 1960s and early 1970s.[82–86] In particular, Terenin *et al.*[82] observed blue fluorescence of a chlorophyll solution excited by a high power ruby laser. Violet fluorescence of an aluminum phthalocyanine chloride solution was studied under similar conditions.[83] It was also found that the action of high-power radiation of a ruby laser on a solution of cyanine dye in methanol leads to the appearance of blue fluorescence with its intensity proportional to the squared exciting radiation intensity.[84] These results were subjected to criticism.[87,88] Blue fluorescence was suggested to be due to photochemical decomposition products of the dye. However, blue fluorescence was also observed in a CW excitation study of cryptocyanine.[89] The authors of this study found that the blue and red fluorescence excitation spectra match each other and the UV absorption spectrum in the UV spectral region. The quantum yield of the blue fluorescence was 10^{-4}.[89]

The potentialities of the stepwise excitation technique for studying fluorescence from higher excited states of complex molecules have been demonstrated in a series of studies by Lin, Topp *et al.*[90–95] They used a dye laser with an output of 0.1 to 0.5 mJ per $\sim$5 ns pulse, pumped by a nitrogen laser operated at a repetition rate of up to 50 Hz. Fluorescence due to transitions from higher excited singlet states was detected using a monochromator and a photomultiplier with synchronous detection (the signal was averaged over 100–300 pulses). To eliminate scattered visible fluorescence, a light filter was placed in front of the monochromator. The advantages of consecutive stepwise excitation over simultaneous excitation by picosecond pulses with the same energy at the same wavelength were demonstrated taking rubrene as an example.

Stepwise excitation experiments can be performed even using a high-power CW laser. For instance, the $S_3 \rightarrow S_0$ fluorescence spectrum of tetracene (a solution in methylcyclohexane) was measured using an Ar laser with an output of 0.8 W at 233 K by focusing the laser light on a flow-through cell.[96] This is the first observation of fluorescence accompanying the transition from HESS of aromatic hydrocarbon molecules under conditions of stepwise excitation.

In studies of $S_n \rightarrow S_0$ fluorescence spectra of rhodamine B and rhodamine 6G (solutions in ethanol) at 300 K Lin and Topp[91] observed three prominent bands in the region 250–400 nm for each compound, at 275, 320 and 382 nm for rhodamine B and at 270, 310 and 377 nm for rhodamine 6G. The shapes of these band systems were found to be nearly mirror images of the three-band systems corresponding to electronic transitions in the absorption spectra of the dyes. The fluorescence band of rhodamine 6G at 377 nm matches that measured in the earlier[85,86] and more recent[97] studies. Polarisation spectrum measurements confirmed the presence of three electronic transitions in the observed fluorescence spectrum. It should be noted that positions of the fluorescence bands of the rhodamines at 382 and 377 nm remain virtually unchanged upon variation of the second quantum frequency from 22 000 to 18 000 cm^{-1}.

Stepwise excitation technique was used to study a large number of aromatic hydrocarbon molecules characterised by several electronic transitions in this spectral region.[92–95] It was shown that electronic relaxation of higher excited singlet states of organic molecules occurs until vibrational equilibration is established after the excitation event. Studies of $S_n \rightarrow S_0$ transitions in the 3,4,9,10-dibenzopyrene molecule revealed the appearance of a fine vibrational structure in the spectral region adjacent to the effective excitation frequency [$\nu_{ef} = \nu_{0-0}(S_1) + \nu_2$] after excitation by the second quantum (540–610 nm). It was found that this fine structure depends on the frequency of the second excitation quantum. The spacing between the observed bands (1460$\pm$60 cm^{-1}) is close to that of the principal progression in the $S_1 \rightarrow S_0$ fluorescence spectrum (1440$\pm$50 cm^{-1}). Topp and Lin[93] suggested that the observed vibrational structure of the spectrum is caused by the anti-Stokes Raman scattering; however, they did not rule out that a phenomenon similar to the Personov effect[98,99] is observed in this case.

Distinctions between the structures of the spectra measured near the excitation level have been found for centrosymmetric molecules and those without a centre of symmetry.[94] Under conditions of two-step excitation, selection rules forbid transitions of centrosymmetric molecules in those states from which radiative transitions to the S_0 ground state are allowed. Indeed, judging from the sum of the $S_1 \leftarrow S_0$ transition frequency and the second absorbed quantum frequency, in this case the fluorescence spectrum begins 'some distance' from its conventional position.

Stepwise excitation studies of a large number of fluorescent dyes and aromatic molecules in solutions at room temperature and at 77 K have been carried out.[100–106] It was found that intramolecular nonradiative transitions from higher excited singlet levels in dyes and most complex aromatic compounds in solutions occur in a cascade manner, *i.e.*, consecutively involving all the lower-lying electronic levels. This conclusion was drawn based on comparison of the shape of fluorescence spectra of organic molecules excited by the second quantum with varied frequency in states with different energies. The $S_n \rightarrow S_0$ ($n \geqslant 2$) fluorescence spectra of Magdale Red dye (a solution in ethanol) at 77 K are shown in Fig. 3 while those of 1,2-benzanthracene (a solution in ethanol) at 293 K are presented in Fig. 4. The spectra shown in Figs 3 and 4 exhibit prominent bands that are mirror images of corresponding $S_n \leftarrow S_0$ absorption bands. In addition, the intensity ratio of the $S_n \rightarrow S_0$ and $S_{n-k} \rightarrow S_0$ bands ($k < n$) remains constant as the energy of the second quantum varies.

The ratio of the areas under the bands corresponding to different $S_n \rightarrow S_0$ transitions characterises the relative quantum yield of a given fluorescence transition. Given the absolute quantum yield of a particular intramolecular transition, it is possible to determine the absolute quantum yields for other transitions. The corresponding radiative rate constant can be found from the area under that absorption band which is the mirror image of the fluorescence band of the given transition. Then, one can estimate the S_n state lifetimes

$$\tau(S_n) = \tau_r(S_n \leftarrow S_0)\, q_{fl}(S_n \rightarrow S_0).$$

Here, $\tau_r(S_n \leftarrow S_0)$ is the inverse of the rate constant for the $S_n \rightarrow S_0$ radiative transition and $q_{fl}(S_n \rightarrow S_0)$ is the fluorescence quantum yield. The fluorescence quantum yields and decay times thus obtained are listed in Table 4.

The results of analysis of the spectra presented in Figs 3 and 4 and those reported elsewhere[97,100–106] are sufficient to allow the following conclusions.

First, stepwise excitation of a molecule to an S_n ($n \geqslant 2$) state leads to the appearance of the spectral bands corresponding to the $S_n \rightarrow S_0$, $S_{n-1} \rightarrow S_0$, $S_{n-2} \rightarrow S_0$, *etc.* transitions in the fluorescence spectrum of the molecule.

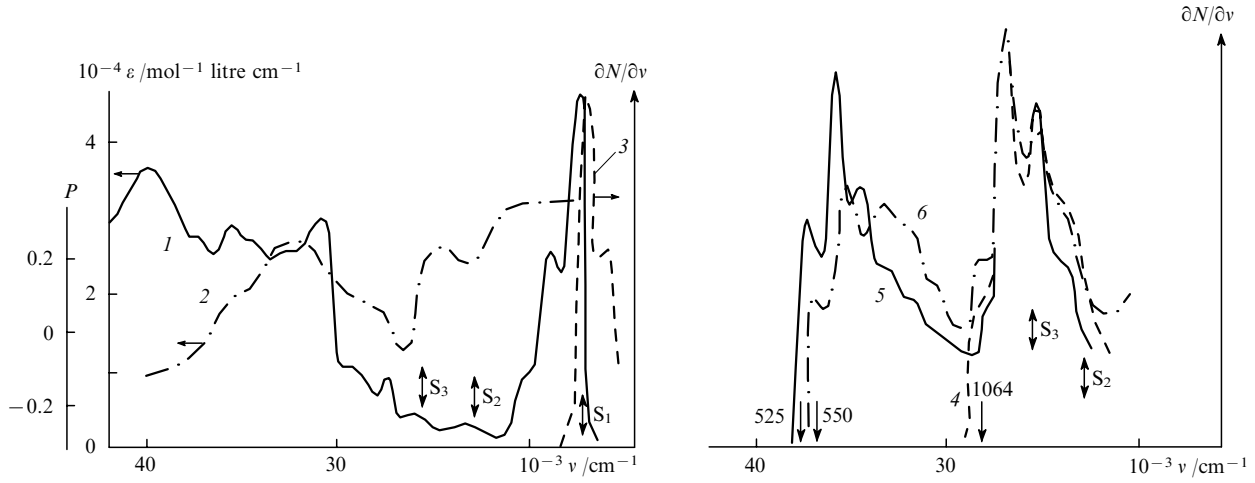


Figure 3. Magdale Red spectra (a solution in ethanol).
The $S_n \leftarrow S_0$ absorption spectrum at 77 K (*1*); polarisation spectrum of $S_1 \rightarrow S_0$ fluorescence excitation as function of excitation frequency at 293 K (a solution in glycerol) (*2*), see also a separate *P* scale; $S_1 \rightarrow S_0$ fluorescence spectrum at 77 K (*3*) and $S_n \rightarrow S_0$ ($n \geqslant 2$) fluorescence spectra (*4–6*) obtained under conditions of stepwise excitation from the S_1 state at λ_{exc} = 1064, 550 and 525 nm, respectively. Double vertical arrows denote the energy levels of S_n electronic states on the frequency scale. Single arrows denote the energy levels achieved under conditions of stepwise excitation. *N* is the number of absorbed quanta.

Second, for most of molecules (except for those characterised by strongly different equilibrium nuclear configurations in the S_1 and S_0 states) each band in the $S_n \leftarrow S_0$ absorption spectrum has a nearly mirror image in the $S_n \rightarrow S_0$ fluorescence spectrum.

Third, if excitation of a molecule by the second quantum leads to population of an upper S_k ($k > n$) state and if the S_n levels are populated by $S_k \rightsquigarrow S_{k-1} \rightsquigarrow S_n$ electronic relaxation, the shape of fluorescence spectra and, in particular, the shape of particular bands corresponding to $S_n \rightarrow S_0$ transitions and the band intensity ratios are in most cases independent of the energy of the second quantum.

Fourth, distortion of the fluorescence spectra from higher excited states is observed only if the total energy of the $S_1 \rightarrow S_0$ transition and the second excitation quantum is larger than the ionization energy of the molecule under study in solution (see Figs 3 and 4).

To obtain additional experimental verification of the assumption of cascade character of intramolecular electronic relaxation, the absolute quantum yields ($q_{fl\,n0}$) of $S_n \rightarrow S_0$ fluorescence were measured at different energies of the second excitation quantum. By the quantum yield of fluorescence due to intramolecular transitions from higher excited electronic states under conditions of stepwise excitation is meant the ratio of the number of the quanta emitted in the form of $S_n \rightarrow S_0$ fluorescence to the number of molecules excited to the S_n state. Determination of $q_{fl\,n0}$ requires knowledge of the number of absorbed (the $S_n \leftarrow S_1$ transition) and emitted ($S_n \rightarrow S_0$ transition) quanta. The former parameter is complicated to calculate. Previously,[97, 100–106] it was estimated

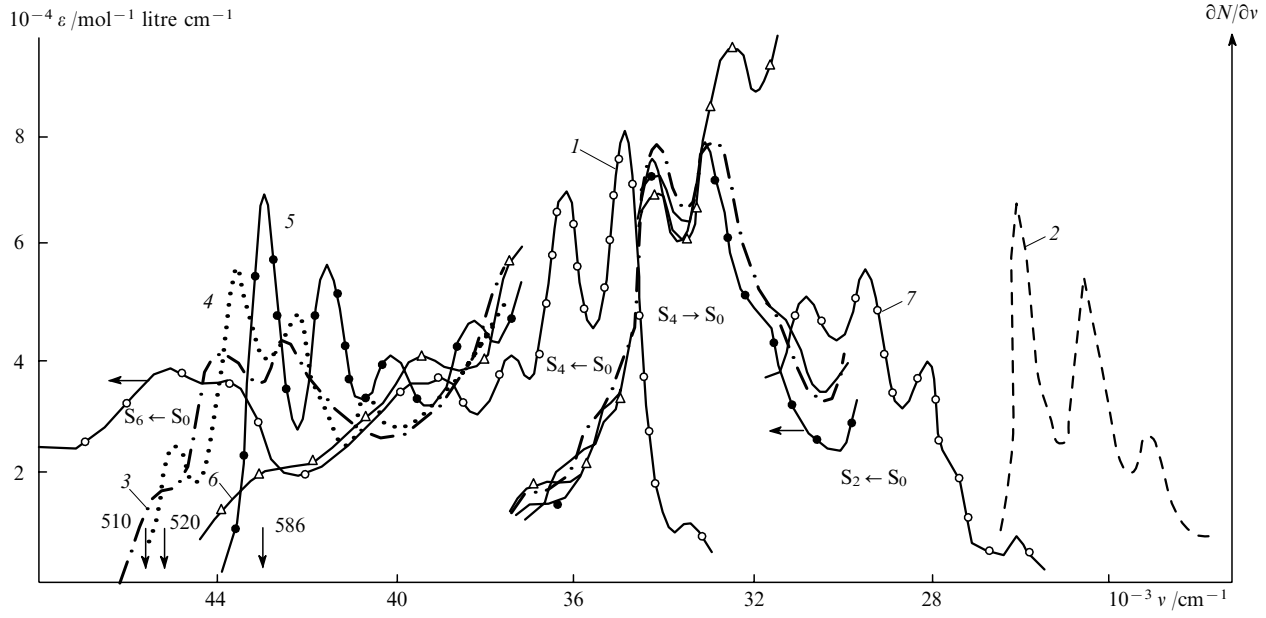


Figure 4. Spectra of 1,2-benzanthracene (a solution in ethanol) at 293 K.[72]
The $S_n \leftarrow S_0$ absorption (*1*) and $S_1 \rightarrow S_0$ fluorescence (*2*) spectra. The $S_n \rightarrow S_0$ ($n \geqslant 2$) fluorescence spectra obtained under conditions of stepwise excitation from the S_1 state at λ_{exc} = 510, 520, 586 and 340 nm, respectively (*3–6*); enlarged representation of the $S_n \leftarrow S_0$ absorption spectrum (*7*) (8 times along the ordinate axis). The spectral width of the instrumental response function was 200 cm^{-1}.

Table 4. Characteristics of transitions from the HESS of organic molecules (fluorescence spectra and yields were measured using stepwise excitation technique).

Compound	n	ΔE_{n0} /cm^{-1}	$\Delta E_{n,n-1}$ /cm^{-1}	$q_{\mathrm{fl}\,n0}$	$k_{\mathrm{r}\,n0}$ /s^{-1}	$k_{\mathrm{nr}}(S_n \rightarrow S_{n-1})$ /s^{-1}	τ_n /ps	Ref.
Solvent — ethanol, 77 K								
Brilliant Green	2	21 800	6300	1×10^{-4}	5×10^{7}	5×10^{11}	2	97
	4	30 600	4500	2×10^{-6}	8.3×10^{7}	4.2×10^{13}	0.024	
Rhodamine B	2	22 800	5100	3×10^{-6}	1×10^{7}	3.3×10^{12}	0.3	97
	3	24 600	1800	4×10^{-6}	1.4×10^{7}	3.6×10^{12}	0.28	
	4	27 700	3100	1×10^{-5}	4×10^{7}	4.0×10^{12}	0.25	
	5	31 800	4100	4×10^{-6}	1.4×10^{8}	3.3×10^{13}	0.03	
Magdale Red	2	23 300	6000	1.5×10^{-6}	8.3×10^{6}	5.6×10^{12}	0.18	97
	3	25 500	2200	4.5×10^{-6}	1.3×10^{7}	3.0×10^{12}	0.33	
Solvent — ethanol, 293 K								
Rhodamine 6G	2	24 300	5600	2×10^{-6}	1×10^{7}	5.0×10^{12}	0.2	97
	3	25 650	–	–	–	–	–	
	4	28 400	2750	1×10^{-5}	5×10^{7}	5.0×10^{12}	0.2	
Pyrene	4	36 300	6000	7×10^{-6}	4×10^{8}	5.0×10^{13}	0.02	97
	5	41 000	4700	1.8×10^{-5}	5×10^{8}	2.9×10^{13}	0.035	
	6	~44 500	~3500	$\sim6\times10^{-6}$	$\sim3\times10^{8}$	$\sim4.5\times10^{13}$	~0.022	
1,2-Benzanthracene	4	34 500	1100	4×10^{-5}	6.7×10^{8}	1.7×10^{13}	0.06	97
	5	38 500	4000	1.3×10^{-5}	5×10^{8}	3.8×10^{13}	0.026	
	6	43 000	4500	1.3×10^{-5}	7×10^{8}	5.6×10^{13}	0.018	
9,10-Di-*n*-propylanthracene	2	37 700	< 3000	3×10^{-5}	1.4×10^{8}	4.3×10^{13}	0.023	107
α-Naphthylphenyloxazole	2	35 300	7800	4×10^{-6}	(1.6×10^{8})	–	(0.024)	104
	3	41 000	5700	5.6×10^{-6}	(6.7×10^{8})	–	(0.010)	
3,4.9,10-Dibenzopyrene	2	25 500	2300	–	–	–	0.2	95
	3	30 100	4600	–	–	–	> 0.1	
	4	34 100	4000	–	–	–	0.08	
	5	37 600	3500	–	–	–	–	
	6	41 500	3900	5×10^{-5}	2.2×10^{9}	–	0.04	

Note. The values estimated from the linewidths in structured fluorescence spectra and unreliable results due to difficulties of the determination of the emission rate constant owing to changes in the molecular configuration in the excited state are given in parentheses.

from changes in the intensity of transmitted laser radiation with the frequency ν_2 upon turning on a laser with the frequency ν_1 and from the amplitude of additional opto-acoustical signal which appeared upon simultaneous illumination of the object under study by two laser pulses.[107]

The fluorescence quantum yield was also estimated [108] from the following relationship

$$q_{\mathrm{fl}\,n0} = \frac{I_{\mathrm{fl}\,n0}}{I_{\mathrm{fl}\,10}\sigma_{1n}I_{\mathrm{ex}\,2}\tau_{\mathrm{r}1}},$$

where $I_{\mathrm{fl}\,n0}$ and $I_{\mathrm{fl}\,10}$ are the integrated intensities of the S_n and S_1 fluorescence, respectively; σ_{1n} is the absorption cross-section for the $S_n \leftarrow S_1$ transition, $I_{\mathrm{ex}\,2}$ is the power density of exciting radiation with the frequency ν_2 and $\tau_{\mathrm{r}1}$ is the radiative lifetime of the S_1 state.

Table 5 lists the results obtained for α-naphthylphenyloxazole, pyrene and 1,2-benzanthracene. As can be seen, the $q_{\mathrm{fl}\,n0}$ values are independent of energy of the second quantum within the experimental error. This is a strong argument in favour of the cascade mechanism of electronic relaxation of HESS.

Let us analyse the spectra of fluorescence accompanying transitions from the HESS of most of the molecules studied, obtained under conditions of stepwise excitation. The following picture is observed in the region adjacent to the frequency corresponding to the sum of the energies of the S_1 state and the second excitation quantum. The $S_n \rightarrow S_0$ fluorescence spectra (S_n is the state directly populated by absorption of the second quantum) exhibit a more pronounced vibrational structure compared to the $S_n \leftarrow S_0$ absorption spectra of the same molecules obtained under the same conditions and to the fluorescence

Table 5. Absolute $S_n \rightarrow S_0$ fluorescence quantum yields ($q_{\mathrm{fl}\,n0}$) measured using stepwise excitation technique.[97, 104]

Compound	ν_1 /cm^{-1}	ν_2 /cm^{-1}	Energy level to be excited	$10^6 q_{\mathrm{fl}\,n0}$ (see [a])	(see [b])
α-Naphthyl-phenyl-oxazole	27500	16 950	S_3	4.0 ± 0.8	5.6 ± 1.5
		18 200	S_3	3.5 ± 0.8	4.9 ± 1.5
		19 250	S_4	4.2 ± 0.8	5.8 ± 1.5
Pyrene	26000	16 950	S_4	3.0 ± 1.0	3.5 ± 1.0
		18 200	S_5	4.0 ± 1.5	4.5 ± 1.5
		19 250	S_6	5.0 ± 2.0	6.0 ± 2.0
1,2-Benz-anthracene	25900	16 950	S_5	35 ± 8	–
		18 200	S_6	35 ± 8	–
		19 250	S_6	35 ± 8	–

Note. Measurements were carried out in ethanol solutions at 293 K.
[a] Given are the $q_{\mathrm{fl}\,20}\times10^6$ values ($\nu_{\max} \approx 33\,200$ cm^{-1}) for α-naphthyloxazole and $q_{\mathrm{fl}\,40}\times10^6$ values ($\nu_{\max} \approx 34\,500$ cm^{-1}) for pyrene and 1,2-benzanthracene; [b] given are the $q_{\mathrm{fl}\,30}\times10^6$ values ($\nu_{\max} \approx 39\,300$ cm^{-1}) for α-naphthyloxazole and $q_{\mathrm{fl}\,50}\times10^6$ values ($\nu_{\max} \approx 41\,500$ cm^{-1}) for pyrene.

spectra from the HESS populated *via* relaxation from higher excited levels (see Figs 3 and 4).

Positions of all the fluorescence bands observed depend on the frequency of the second quantum. On the other hand, neither the structure nor the relative intensities of the fluorescence bands corresponding to transitions from the lower-lying HESS populated *via* relaxation remain unchanged (see curves *4–6* in Fig. 3 and curves *4* and *5* in Fig. 4).

If the frequency of the second excitation quantum varies within $\Delta\nu_2 < 1500\ cm^{-1}$, the entire spectral region in question (it will be remembered that this is a region of the fluorescence spectrum) is shifted simultaneously with the position of the level to be populated. An increase in $\Delta\nu_2$ leads to substantial redistribution of vibronic band intensities. Further increase in the frequency ν_2 (by several thousands of cm^{-1}) causes the appearance of spectral bands corresponding to emission of nearly the same intensity; however, the new bands exhibit no pronounced vibrational structure.

The appearance of structured $S_n \rightarrow S_0$ fluorescence spectra can probably be rationalised by the effect of selective excitation of molecules with a particular configuration into a broad $S_n \leftarrow S_0$ absorption band by spectrally narrow ($\sim 0.5\ cm^{-1}$) radiation with the frequency ν_2. Due to ultrashort lifetimes of the S_n states (10–100 fs) of those molecules which exhibit structured spectra, inhomogeneous line broadening in the $S_n \leftarrow S_1$ absorption spectrum can be considered as manifestation of specific molecular conformations due to low-frequency, out-of-plane vibrations of the aromatic rings.

This explanation is also supported by the fact that Brilliant Green and Zn-tetrabenzoporphyrin exhibit no structured spectra upon excitation of the relatively long-lived ($\sim 1-3$ ps) S_2 state. On the other hand, stepwise excitation of Brilliant Green by the second quantum ($\lambda_2 = 500-620$ nm) and population of the S_5 level ($\tau_5 \leqslant 24$ fs) leads to the appearance of a structured spectrum. This is consistent with the assumption that the structured spectra are observed upon transitions from electronically and vibrationally unrelaxed states, while the excited states with the picosecond lifetimes undergo at least partial vibrational relaxation.

It was assumed [97, 103] that the effect in question (the appearance of structured spectra) is to some extent similar to the Personov effect, *i.e.*, the appearance of the $S_1 \rightarrow S_0$ fluorescence spectra with well-resolved fine structure under the action of selective laser excitation of organic molecules in solid solutions at 4 K (see Refs 98 and 109).

There are some distinctions between these effects. First, a structured spectrum appears in the case where one electronic transition ($S_n \leftarrow S_1$) is selectively excited while another transition ($S_n \rightarrow S_0$) is used for the detection of structured emission. Conventional Personov effect is not observed in this situation since the two transitions are uncorrelated. Second, structured spectra are observed in liquid solutions without cooling them down to the liquid helium temperature (though liquid solutions can be considered as solid ones during a time of the order of tens of femtoseconds). Third, corresponding vibronic levels are noticeably broadened (up to hundreds of cm^{-1}) due to the short lifetimes of the excited states, whereas in the case of the Personov effect the linewidths are equal to hundredth and thousandth fractions of cm^{-1}. Finally, structured spectra appeared under conditions of stepwise excitation are observed only for those molecules for which the 0–0 band of the $S_1 \rightarrow S_0$ transition is only slightly inhomogeneously broadened.

The appearance of a structured fluorescence spectrum under conditions of stepwise excitation was explained in another manner.[110] The authors of this study assumed that the observed fluorescence is due to anti-Stokes resonant vibronic Raman scattering (ARVRS). An energy level diagram illustrating the proposed [110] formation mechanism of structured emission spectrum is shown in Fig. 5. ARVRS occurs if excitation of a molecule to the S_1 state after absorption of the first quantum is followed by absorption of the second excitation quantum with the frequency ν_2. As a result, transition of the molecule to a vibrational electronic ground-state level is accompanied by scattering of a quantum corresponding to the frequency $\nu_2 + \nu_{0-0}(S_1-S_0) - \Sigma n_i \nu_i$. Later, the authors of other studies [108, 111, 112] supported this explanation and pointed to the similarity of the observed spectrum and the usual fluorescence spectrum shifted towards the high-frequency region.

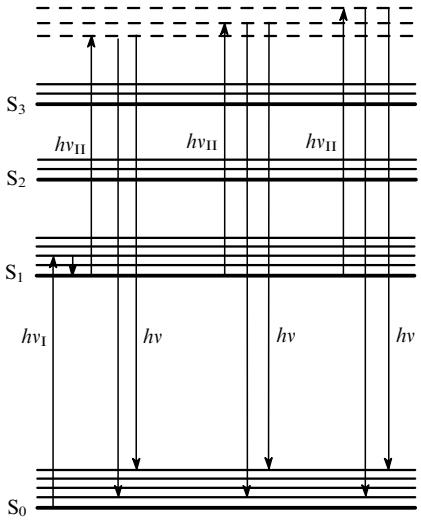


Figure 5. An energy level diagram illustrating the ARVRS mechanism. Dashed lines denote virtual energy levels involved in the Raman scattering. Vertical lines corresponding to ARVRS are denoted as *hν*.

Nevertheless, we dissent from the proposed [110] explanation for the experimental observations. Let us adduce some arguments in favour of the interpretation of structured emission appearing under conditions of stepwise excitation of organic molecules as fluorescence.

If an excited level is populated *via* relaxation from upper levels rather than by direct excitation, the integrated intensity of the structured spectrum is nearly the same as the emission intensity in the same spectral region.[97]

The bands in the structured spectrum are much broader than those in the $S_1 \rightarrow S_0$ fluorescence spectrum. On the other hand, the ARVRS mechanism requires that the width of the short-wavelength band in the structured spectrum obtained under conditions of stepwise excitation and the width of the 0–0 band in the $S_1 \rightarrow S_0$ fluorescence spectrum be equal.

If a molecule in the S_1 state is excited by a second quantum and if the energy of this quantum is sufficiently high for the molecule to undergo photoionisation, the fluorescence yield from higher excited states should decrease dramatically. It is just the situation that is observed in the experiments. For instance, in the case of rhodamine B the fluorescence yield from HESS decreases by more than an order of magnitude as the frequency ν_2 is varied from $19\,000\ cm^{-1}$ to $\nu_2 > 32\,000\ cm^{-1}$. Assuming that structured emission is due to ARVRS, there is no grounds for such a large decrease in the emission intensity, since the process involves only virtual high-lying states.

Nonradiative energy transfer from a higher excited state of 1,2-benzanthracene, which was stepwise excited to the region of structured spectrum, to benzene and xylene molecules has been observed.[112] This transition was interpreted as ARVRS. However, the authors of this study noted that nonradiative energy transfer from the virtual levels involved in ARVRS is rather strange.

The problem of 'hot' fluorescence bands in emission spectra due to transitions from HESS has been considered.[113] If a molecule excited to an upper singlet state by the second quantum relaxes to a lower-lying HESS, a substantial excess vibrational energy is stored in the latter state. Hence, it is logical to expect the appearance of 'hot' fluorescence bands in the emission spectrum from this state. If the HESS lifetimes are shorter than the time of vibrational energy redistribution within a complex molecule, the intensities of 'hot' fluorescence bands are determined by the population probability of the states in question *via* internal conversion from upper electronic states and by the rate of the initial stage of energy exchange between the optically active and inactive vibrations. At first glance, the intensities of 'hot' bands in

the emission spectrum must be strongly dependent on the excess vibrational energy in the emitting S_n ($n > 1$) state and, hence, on the energy of the second quantum. However, as can be seen in Fig. 4, the $S_4 \rightarrow S_0$ fluorescence bandshape of 1,2-benzanthracene depends only slightly on the second-quantum energy when it is varied from 17 100 to 28 200 cm^{-1} (for the S_4 state, this corresponds to an excess vibrational energy lying between 8400 and 19 500 cm^{-1}). Considering a 'hot' fluorescence band lying 1400 cm^{-1} above the 0–0 band of the $S_4 \rightarrow S_0$ transition, Lyubimtsev [113] has come to the conclusion that cascade relaxation passes through an optically active vibrational state (1400 cm^{-1}) with a unit probability.

IV. Lifetimes of higher excited S_n states estimated from fluorescence quantum yields and absorption integrals

Determination of a HESS lifetime requires knowledge of the ratio of absolute quantum yield of $S_n \rightarrow S_0$ fluorescence to the number of absorbed second quanta and the radiative rate constant for the same transition. The latter parameter can be estimated using the absorption integral for the band corresponding to the $S_n \leftarrow S_0$ transition.[114, 115]

$$\tau_n = \frac{q_{\mathrm{fl}\,n0}}{k_{\mathrm{r}\,n0}}.$$

A number of studies concerning this subject have been reported.[97, 100, 106] It was found that the HESS lifetimes of organic molecules in solutions vary from several picoseconds for the S_2 states of certain molecules to 10–20 fs for the S_n states, $n = 3–6$. The τ_n values of the order of tens of femtoseconds mean that the electronic relaxation rates of these states are higher than the intramolecular vibrational relaxation rates which were estimated at hundreds of femtoseconds.[19, 116, 117] Elsaesser and Kaiser [20] proposed to distinguish between two types of vibrational excitation relaxation, *viz*., fast relaxation for the energy redistribution between isoenergetic vibrational states and slow relaxation corresponding to the relaxation to lower-lying energy levels. Transfer of excess vibrational energy from the molecule under study to the environment (solvent molecules) proceeds at lower rates and is characterised by the times of the order of several tens of picoseconds.[19, 116] Therefore, the cascade relaxation of the HESS of organic molecules (except for the S_2 state of a certain molecules) can be considered as occurring with conservation of the energy supplied to the molecules. Variation of the excess vibrational energy was found to have a slight effect on the band position and shape in the $S_n \rightarrow S_0$ fluorescence spectra, though in some cases this energy was varied by 10 000 cm^{-1} and more.

Electronic relaxation times of the HESS of aromatic and dye molecules are nearly equal to the period of optically active vibrations ($\nu = 1200–1600$ cm^{-1}) or even shorter.

To verify such interesting results, attempts have been undertaken at estimating the HESS lifetimes using other methods. For instance, the τ_v values were found from the line broadening in the structured spectra appearing upon selective excitation by the second quantum of the HESS lying near the initially excited state.[97, 104] The spectral widths of vibronic bands (the first vibronic band) in such spectra were compared with the spectral width of the 0–0 band in the usual fluorescence spectrum. In those cases where the 0–0 bands were only slightly inhomogeneously broadened (pyrene, 1,2-benzanthracene, phenanthrene, $T = 77$ K), the structured spectra were additionally broadened. Assuming that the broadening of the upper (S_n) and lower (S_1, S_0) levels is uncorrelated, the broadening $\Delta\nu'_{n0}$ due to the short lifetime of the S_n state (*i.e*., the homogeneous width) was estimated using the formula

$$\Delta\nu'_{n0} = \sqrt{[\Delta\nu_{n0}(S_n - S_0)]^2 - [\Delta\nu_{10}(S_1 - S_0)]^2},$$

where $\Delta\nu_{v0}$ and $\Delta\nu_{10}$ are the halfwidths of the corresponding bands.

The broadening calculated using this formula (300 cm^{-1} for the S_6 states of pyrene and 1,2-benzanthracene) corresponds to the lifetime of these states, $\tau_6 = 18$ fs.

These τ_6 values are in reasonable agreement with the estimates obtained for pyrene ($\tau_6 = 15–30$ fs) and 1,2-benzanthracene ($\tau_6 = 18$ fs) from the absolute quantum yields of fluorescence.

The rate constants for nonradiative transitions between the HESS are calculated using the absolute quantum yields of the $S_n \rightarrow S_0$ fluorescence and the radiative rate constants estimated from the band integral in the $S_n \leftarrow S_0$ absorption spectrum. It should be noted that the results of calculations of the absorption band integral refer to the molecule which is in the S_0 state and has its equilibrium configuration. However, the molecule excited from the S_1 state to a HESS after absorption of the second quantum retains the configuration of the former state. If the equilibrium molecular configurations in the S_1 and S_0 states differ only slightly, these estimates of τ_v are justified. However, in some cases (*e.g*., *p*-terphenyl or 2,5-diphenyloxazole) the molecular configuration in the excited (S_1) state is substantially different from the ground-state (S_0) configuration. This manifests itself in different patterns of their absorption and usual fluorescence spectra. According to X-ray diffraction data, the ground-state structure of the *p*-terphenyl molecule is nonplanar.[118] On the other hand, quantum-chemical calculations [119] showed that in the case of fluorescence emission this molecule has a nearly planar configuration. Clearly, the oscillator strengths of electronic transitions and the corresponding energy levels can vary over a wide range upon changes in the molecule geometry (Fig. 6).

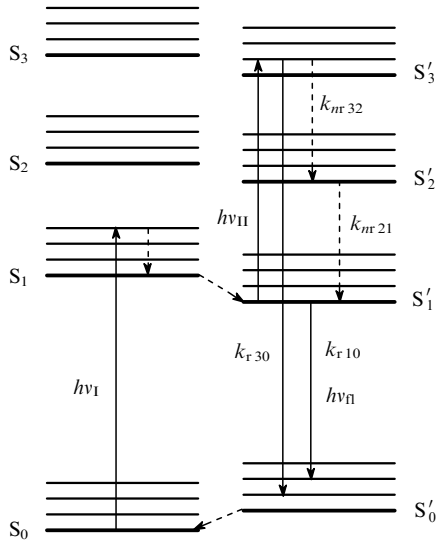


Figure 6. An energy level diagram illustrating two-quantum stepwise excitation of a molecule in the case of variations of the molecular configuration or solvate environment during the lifetime of the fluorescent (S_1) state. The energy levels belonging to the triplet manifold are not shown.

V. Delayed fluorescence from higher excited S_n states due to triplet–triplet annihilation

As has been shown experimentally,[120] annihilation of two molecules being in the lowest triplet state (the so-called triplet–triplet annihilation) can lead to generation of both the first and upper excited singlet (and triplet) states of the molecules:

$$T_1 + T_1 \rightarrow S_n + S_0, \; n \geqslant 1.$$

This process leads to the appearance of not only the usual $S_1 \rightarrow S_0$ fluorescence, but also the $S_n \rightarrow S_0$ ($n > 2$) delayed fluorescence due to triplet–triplet annihilation. This feature was used to detect the phenomenon in question. The first successful experiments were carried out taking 1,2-benzanthracene and fluoranthene dissolved in paraffin oil as examples. A schematical energy level diagram of the interacting molecules is shown in Fig. 7.

Triplet–triplet annihilation studies of a number of aromatic compounds, *e.g.*, naphthalene (S_2), phenanthrene (S_3), triphenylene (S_3), 1,2-benzanthracene (S_3), pyrene (S_2), chrysene (S_3), fluoranthene (S_4) and *N*-methylcarbazole (S_4, S_2?), anthraquinone (S_3, S_4), xanthone (S_3) have been carried out.[121–124] (The singlet state generated after triplet–triplet annihilation is given in parentheses.)

Triplet–triplet annihilation induced fluorescence from the HESS is observed using a phosphoroscope. This allows effective suppression of the stray exciting light, though the usual fluorescence light [it is nearly four orders of magnitude more intense than the $S_n \rightarrow S_0$ ($n \geqslant 1$) fluorescence] remains. In contrast to the stepwise excitation method, triplet–triplet annihilation technique does not allow variation of the energy of the second quantum over a wide range. However, in the former case it is difficult to observe the region near the short-wavelength limit of the usual fluorescence in the fluorescence spectra from HESS, since this spectral region is, as a rule, used for excitation of the molecule under study to the S_1 state by the first quantum. As a result, the stray light precludes measurements of the weak $S_n \rightarrow S_0$ ($n \geqslant 1$) fluorescence spectrum. Triplet–triplet annihilation techniques provides much better conditions for the observation of this spectral region (Fig. 8).

Delayed fluorescence spectra of 1,2-benzanthracene, fluoranthene, pyrene and chrysene solutions in methylcyclohexane at 193 K were obtained by triplet–triplet annihilation technique and corrected for the quantum spectral sensitivity of the experimental setup.[121] All the above-mentioned compounds exhibit clearly seen

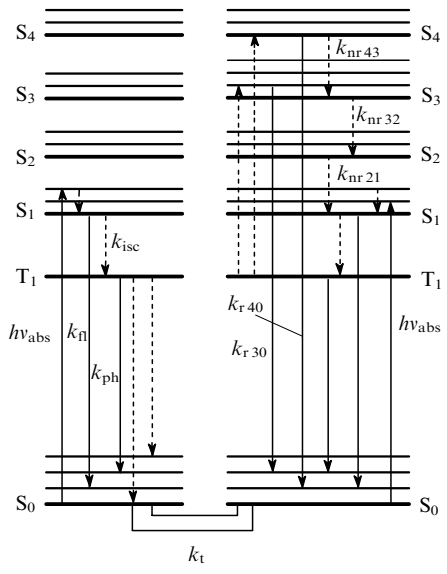


Figure 7. Schematic representation of energy level diagram for nonradiative transitions between higher excited singlet states of a molecule (fluorescence corresponding to transitions from the HESS to the ground state due to triplet–triplet annihilation). Vertical solid and dashed lines denote radiative and intramolecular nonradiative transitions, respectively. The system of dashed lines linked by upward-looking brackets (see the bottom of the diagram) corresponds to the interaction between two triplet molecules accompanied by energy transfer from one to the other molecule and excitation of the latter to a higher excited singlet state (k_t). The energy level diagram for the system of higher excited triplet states of the molecules and the scheme illustrating their triplet–triplet annihilation induced excitation are not shown.

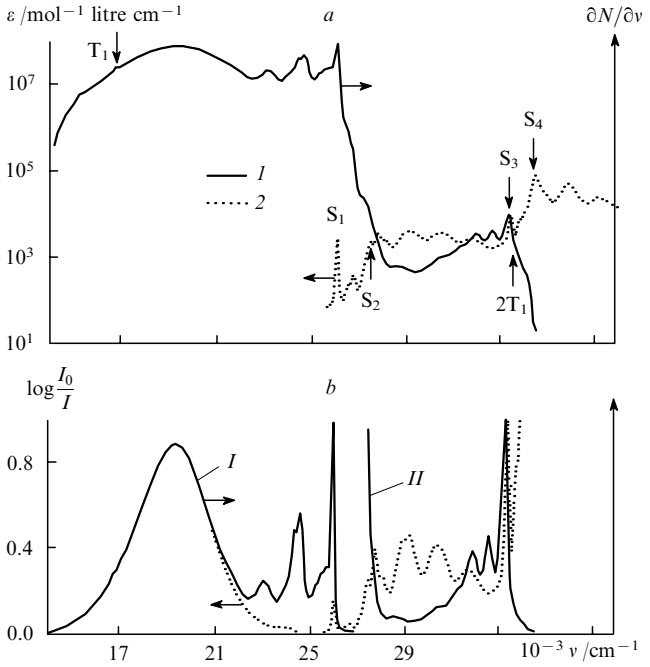


Figure 8. Spectrum of delayed fluorescence due to triplet–triplet annihilation (*1*) and absorption (*2*) spectrum of 1,2-benzanthracene (a 5×10^{-5} mol litre^{-1} solution in methylcyclohexane) measured at $\lambda_{exc} = 365–366$ nm ($T = 193$ K) (I_0 is the initial intensity).
The 'as-measured' (*I*) and expanded (9150 times along the ordinate axis, *II*) representation of the spectra.[121]

$S_n \rightarrow S_0$ fluorescence spectra. In some instances, the $S_n \rightarrow S_0$ fluorescence band appears to be a mirror image of the $S_n \leftarrow S_0$ absorption band, as in the stepwise excitation studies.

$S_n \rightarrow S_0$-Fluorescence spectra of *N*-methylcarbazole (NMC) dissolved in heptane and toluene (Tol) have been studied.[123] Triplet–triplet annihilation was found to induce both fluorescence from HESS of the NMC molecules and sensitised fluorescence of toluene, which is due to the nonradiative energy transfer from the HESS of *N*-methylcarbazole to the toluene molecule. This process can be schematically described as follows:

$$T_1(\text{NMC}) + T_1(\text{NMC}) \rightarrow S_n(\text{NMC}) + S_0(\text{NMC}),$$

$$S_n(\text{NMC}) \rightarrow S_0(\text{NMC}) + h\nu_{fl},$$

$$S_n(\text{NMC}) + S_0(\text{Tol}) \rightarrow S_0(\text{NMC}) + S_1(\text{Tol}),$$

$$S_1(\text{Tol}) \rightarrow S_0(\text{Tol}) + h\nu_{sens\ fl}.$$

Triplet–triplet annihilation of Cd-tetrabenzoporphyrin molecules also induces delayed fluorescence from the S_2 state.[125] In this case, the triplet state was sensitised by triplet–triplet energy transfer from Pd-tetraphenylporphyrin molecules which exhibit only weak S_2 fluorescence [$q_{fl}(S_2 \rightarrow S_0) < 10^{-5}$].

Hetero-triplet–triplet annihilation of azulene and fluoranthene solution in isopentane leads to the appearance of fluorescence from the second excited singlet level of azulene.[126, 127] These studies allowed the determination of the lifetime of the lowest triplet state for azulene (48 μs) and the quantum yields of intersystem crossing for this molecule, $q(S_1 \rightarrow T_1) = 4 \times 10^{-6}$ and $q(S_2 \rightarrow T_1) = 4 \times 10^{-2}$. The rate constants for intersystem crossing, corrected for the lifetimes of azulene molecule in the S_1 and S_2 states (see Table 1), were found to be $k(S_1 \rightsquigarrow T_1) = 2 \times 10^6$ s^{-1} and $k(S_2 \rightsquigarrow T_1) = 2.8 \times 10^7$ s^{-1}. Delayed $S_2 \rightarrow S_0$ fluorescence of 4,6,8-trimethylazulene due to homo-triplet–triplet annihilation was observed[128] at 27 680 cm^{-1} using sensitisation of triplet states by adding phenazine to the solution (the T_1 energy is 15 630 cm^{-1}). Hetero-triplet–triplet annihilation of anthracene and xanthone molecules was used[129] to study fluorescence from the S_6 ($^1B_{3u}^+$) level of anthracene, perdeuterated anthracene and

9,10-dimethylanthracene in their solutions in 1,1,2-trichlorotrifluoroethane. The intensity ratio of the $S_6 \rightarrow S_0$ fluorescence to the $S_1 \rightarrow S_0$ usual fluorescence was found to be $\sim 10^{-6}$. Triplet–triplet annihilation of biphenylene (an antiaromatic compound) sensitised with *N*-methylcarbazole in an isopentane–cyclopentane mixture at 178 K allowed the detection [130] of very weak $S_2 \rightarrow S_0$ fluorescence of this compound, which was not previously observed using direct excitation techniques (see Section II). This indicates a rather high sensitivity of the triplet–triplet annihilation method.

A method was proposed for increasing the intensity ratio of the fluorescence from the HESS and usual fluorescence.[123] It involves the addition of quenchers of the S_1 state to the solution under study. The potentialities of this method were demonstrated taking delayed fluorescence due to triplet–triplet annihilation of pyrene in the presence of efficient quenchers (diethylaniline and triethylamine) as an example. (The additives should be efficient quenchers of the lowest excited singlet state rather than the triplet state and be transparent to delayed $S_n \rightarrow S_0$ fluorescence due to triplet–triplet annihilation. They should also not enter into photochemical reactions with the compound under study.) This experimental technique was used in precise measurements of the $S_2 \rightarrow S_0$ fluorescence spectrum of pyrene.[123]

Interesting results were obtained [56] in studies of annihilation delayed fluorescence of 4*H*-1-benzopyran-4-thione (BPT) in perfluoro-1,3-dimethylcyclohexane. The experimentally determined probability of generation of the S_2 state by triplet–triplet annihilation was found to be 0.03. This is much lower than the statistical coefficient for the creation of a singlet state by triplet–triplet annihilation (0.25), obtained assuming that the quintet state is inaccessible from 'energy' considerations. The authors of this study mentioned that the probability obtained (0.03) is of the same order of magnitude as the known parameters for anthracene (0.08) and phenanthrene (0.02). The observed generation of the S_2 state of BPT by triplet–triplet annihilation was interpreted [56] as a special case of Förster's (exchange-resonance) energy transfer mechanism.‡ However, the lack of data on the $T_1 \rightarrow S_n$ absorption spectra of BPT precludes calculations of S_2 generation. Note that exchange-resonance mechanism of energy transfer between T_1 states should be common to processes of generation of both S_n and T_n states and that in the case of similar intensities of the spin-allowed and spin-forbidden transitions in the BPT molecule the $T_1 \rightarrow S_n$ spectra are indistinguishable from the $T_1 \rightarrow T_n$ ones.

The HESS lifetimes were estimated from the broadening of the 0–0 vibronic bands in the absorption spectra compared to the 0–0 band of the long-wavelength transition. Another method used for estimating the τ_v values involved the determination of (i) the quantum yield ratios of $S_n \rightarrow S_0$ fluorescence and delayed $S_1 \rightarrow S_0$ fluorescence under the same conditions and (ii) the rate constants for radiative $S_n \rightarrow S_0$ transitions from the absorption integrals for the corresponding $S_n \leftarrow S_0$ transitions. The estimates obtained are listed in Table 6.

Triplet–triplet annihilation technique has a drawback consisting in uncertainty in the identification of the annihilation-generated HESS, since the excitation probability distribution of these states is determined by the overlap integral of the $T_1 \rightarrow S_0$ emission and $S_n \leftarrow T_1$ absorption spectra normalised to a unit band area. Unfortunately, if the phosphorescence spectra are, as a rule, known, almost no information on the $S_n \leftarrow T_1$ absorption spectra is available. In the case of triplet–triplet annihilation, intersystem crossing becomes allowed in the $S_n \leftarrow T_1$ transitions; however, the effect of the Franck–Condon factors persists.[131]

Katoh and Kotani [132] studied fluorescence from the HESS of an anthracene crystal upon fusion of two singlet (S_1) excitons. They also investigated [133] $S_n \rightarrow S_0$ fluorescence of an anthracene crystal using a two-step laser excitation technique.

‡ Eisenberger *et al.*[56] pointed out that triplet–triplet annihilation of aromatic hydrocarbon molecules follows the exchange-resonance energy transfer mechanism. They used a much higher rate constant for the $T_1 \rightarrow S_0$ transition in BPT.

Table 6. Characteristics of transitions from the HESS of organic molecules.

Compound	n	ΔE_{n0} /cm^{-1}	$\Delta E_{n,n-1}$ /cm^{-1}	$q_{\mathrm{fl}\,n0}$	$k_{\mathrm{r}\,n0}$ /s^{-1}	k_{nr} ($S_n \rightarrow S_{n-1}$) /s^{-1}	τ_n /ps	Ref.
Solvent — isopentane–methylpentane mixture, T = 4 K								
Phenanthrene	2	33 900	5000	–	–	1.3×10^{13}	(0.08)[a]	144
	2	–	–	–	–	–	(0.5)[b]	146
Solvent — methylcyclohexane, T = 190 K								
Pyrene	2	29 600	2600	3.5×10^{-5}	3.8×10^{8}	1.1×10^{13}	0.09	123
	2	–	–	–	–	2.5×10^{13}	($\geqslant$0.04)	123
	4	36 300	6000	7×10^{-6}	4×10^{8}	5.0×10^{13}	0.02	123
Solvent — methylcyclohexane, T = 193 K								
1,2-Benzanthracene	3	33 400	5580	5.5×10^{-6}	4.2×10^{7}	7.7×10^{12}	0.13	121
Fluoranthene	4	34 700	3700	1.1×10^{-5}	4×10^{8}	3.8×10^{13}	0.026	121
	4	–	–	–	–	$\sim 2.0 \times 10^{13}$	($\sim$0.05)	121
Chrysene	3	36 800	6000	1.9×10^{-5}	10^{9}	5.3×10^{13}	0.019	121
	3	–	–	–	–	$\sim 5.9 \times 10^{13}$	($\sim$0.017)	121
Solvent — 1,1,2-trichloro-1,2,2-trifluoroethane, T = 243 K								
Anthraquinone	3	36 500	7000	10^{-5} (see [c])	–	–	–	124
	4	40 000	3500	–	–	–	–	124
Xanthone	3	35 000	5700	10^{-6} (see [c])	–	–	–	124

Notes. Decay times and rate constants of nonradiative transitions were obtained by triplet–triplet annihilation technique. The values estimated from the linewidths in structured spectra are given in parentheses.
[a] At 4 K, [b] in a supersonic jet, [c] experimental conditions: $c = 10^{-5}$ mol litre^{-1}, deoxygenated.

VI. Lifetimes of higher excited S_n states of molecules estimated from homogeneous broadening of absorption spectra

The method of estimation of the HESS lifetimes from the data on homogeneous line broadening in absorption spectra is based on the uncertainty relation, which relates the lifetime of an excited electronic or vibronic state of a molecule under study to the homogeneous broadening of the corresponding energy level

$$\tau_n = \frac{1}{2\pi c \Delta\nu_{1/2}},$$

where, τ_n is the lifetime of the energy level (in seconds), c is the velocity of light (in cm s^{-1}) and $\Delta\nu_{1/2}$ is the halfwidth of the energy level (in cm^{-1}). At first glance, τ_n values can be simply determined using this formula after measuring any absorption or emission line corresponding to the transition between the ground and excited states. Indeed, since the ground-state lifetime is infinitely long, this state contributes negligibly to the homogeneous broadening of the spectrum. However, there is also inhomogeneous broadening, which much exceeds the homogeneous broadening in the case of solutions, and the broadening due to phase relaxation.[134]

Subsequently several experimental methods for elimination or strong suppression of inhomogeneous broadening were developed.[135–142] These are as follows:

— low-temperature measurements of absorption and luminescence spectra of crystals;

— measurements of impurity spectra from crystals in those cases where the impurity molecule under study can be easily incorporated into the unit cell of the matrix crystal (*e.g.*, a naphthalene molecule in durene crystal);

— spectral line narrowing in Shpolskii matrices;

— obtaining of narrow fluorescence spectra using the Personov effect upon excitation to the region of the 0–0 electronic transition by monochromatic radiation;

— 'hole burning' in absorption spectra using photochemical reactions or another mode-selective technique for removal of 'inhomogeneously broadened' molecules with specified electronic energy;

— obtaining of extremely narrow absorption or fluorescence spectra in free supersonic jets.

Narrowing of spectral lines broadened due to phase relaxation is achieved by cooling the samples under study. Therefore, the above-mentioned experimental methods are, as a rule, applicable at temperatures close to the liquid helium temperature. Ignoring phase relaxation requires preliminary measurements and analysis of the temperature dependence of linewidths.

Hochstrasser and Marzzacco[134] studied the $T_n \leftarrow S_0$ and $S_n \leftarrow S_0$ absorption spectra of a number of aromatic compounds in the crystalline phase at 4.2 K. Presumably, they were the first who considered substantial broadening of vibronic bands in the absorption spectra upon excitation to the second and upper electronic states. For instance, marked broadening of vibronic lines was found in the spectra of pyrazine and its derivatives, phenazine, 9,10-diazaphenanthrene, naphthalene and its halogen derivatives in the region of the $T_2 \leftarrow S_0$ transition. According to Kasha's rule, excitation of a molecule to the second triplet state should be followed by fast internal conversion to the lowest triplet state. A similar broadening was observed in the singlet–singlet absorption spectra of naphthalene and quinoxaline molecules incorporated into durene crystals, of naphthalene and quinoxaline vapours and of naphthaldehyde. These spectra exhibited narrow $S_1 \leftarrow S_0$ absorption lines which were substantially broadened on approaching the lines corresponding to the $S_2 \leftarrow S_0$ transition.

Studies of vibronic absorption linewidths of different singlet–singlet transitions of anthracene, coronene and 1,2-benzperylene in Shpolskii matrices revealed[135] noticeable narrowing of the $S_n \leftarrow S_0$ ($n \geqslant 1$) lines with a decrease in the temperature from 300 to 77 K. Further reduction of temperature down to 4.2 K was found to have little effect on the linewidths. Narrowing of the $S_1 \leftarrow S_0$ line was followed down to 4.2 K. The linewidths for a number of compounds are listed in Table 7. However, the $S_1 \leftarrow S_0$ linewidths were found to be strongly overestimated since the S_1 state lifetimes of the molecules under study estimated from these linewidths are nearly three orders of magnitude shorter than the

Table 7. HESS lifetimes of organic molecules estimated from vibronic bandwidths.

Compound	Matrix	T /K	$S_n \leftarrow S_0$	ν /cm^{-1}	Homogeneous linewidth /cm^{-1}	τ_n /ps	Method	Ref.
Anthracene	n-hexane	4.2	$S_1 \leftarrow S_0$	26 234	6.2	0.08	Shpolskii effect	135
	"	77	$S_2 \leftarrow S_0$	39 140	280	0.019	the same	135
	"	77	$S_3 \leftarrow S_0$	45 080	400	0.013	"	135
Coronene	n-heptane	4.2	$S_1 \leftarrow S_0$	23 450	2.1	2.6	"	135
	"	4.2	$S_2 \leftarrow S_0$	28 440	4.1	1.3	"	135
	"	77	$S_3 \leftarrow S_0$	32 870	300	0.018	"	135
	"	77	$S_5 \leftarrow S_0$	46 600	350	0.015	"	135
1,12-Benzoperylene	n-hexane	4.2	$S_1 \leftarrow S_0$	24 636	2.4	2.2	"	135
	"	77	$S_2 \leftarrow S_0$	25 800	420	0.013	"	135
	"	77	$S_5 \leftarrow S_0$	44 580	1400	0.004	"	135
	"	77	$S_6 \leftarrow S_0$	47 100	800	0.007	"	135
Zn-Tetraphenyl-porphyrin	poly(methyl methacrylate)	4	$S_2 \leftarrow S_0$	23 600	7.8	1.4[a]	hole burning technique	141
	poly(vinyl butyral)	4	$S_2 \leftarrow S_0$	23 480	6.5	1.6	the same	141
	see[b]		$S_2 \leftarrow S_0$	25 120	4.0	1.3	supersonic jet	142
Zn-Tetratolyl-tetrabenzo-porphyrin	"	20	$S_2 \leftarrow S_0$	?	6.1	1.7	the same	141
Tetrabenzopor-phyrin derivative	THF–Et_2O	4.2	$S_2 \leftarrow S_0$	16 500	25	0.2	hole burning technique	140
	(1 : 1) mixture	4.2	$S_3 \leftarrow S_0$	23 040	11	0.48	the same	140
Free porphyrin base	see[b]	–	$S_2 \leftarrow S_0$	19 884	11	0.48	supersonic jet	142

[a] From fluorescence yields, [b] vapour in a supersonic jet.

measured lifetimes. Analysis of the results obtained in the above-mentioned studies [136–139] shows that these linewidths much exceed the natural linewidths even in the Shpolskii matrices; determination of the natural linewidths requires the Personov holes [98, 99] to be 'burnt' in the absorption lines.

The linewidths of transitions to upper excited singlet states also seem to be overestimated.

A series of studies on free porphyrin base dissolved in the Shpolskii matrices has been reported.[136–139] The homogeneous linewidths were determined using a photochemical hole burning technique based on the tautomeric transformations involving inner hydrogen atoms of the porphyrin molecule.[64, 136] Samples were irradiated by a tunable single-mode laser with a frequency jitter of $\sim$10 MHz. The contribution of phase relaxation was determined from the temperature dependences of the 0–0 linewidths in the range from 1.5 to 4.2 K. The homogeneous width of the 0–0 line for the $S_1 \leftarrow S_0$ transition was found to be $\sim$9 MHz (0.0003 cm^{-1}) at 1.5 K,[137] which corresponded to the experimentally observed $S_1 \leftarrow S_0$ fluorescence decay time of free porphyrin base in n-octane at 4.2 K (17 ns). This indicates that the hole burning technique does allow measurements of homogeneous line broadening, thus providing a means for determination of the lifetimes of the excited states of organic molecules.

The lifetimes of vibronic levels for the S_1 state of free porphyrin base in n-octane at 4.2 K (Table 8) were determined using the same procedure.[139] The homogeneous holewidth of the 0–0 band was found to be $\sim$9 MHz, whereas those of the vibronic bands for the same transition were varied from 5 to 150 GHz (0.1–7 cm^{-1}). Both hole burning and measurements of vibronic bandwidths in the spectra corresponding to transitions to upper electronic excited levels were performed using a tunable pulsed laser with a bandwidth of $\sim$1 cm^{-1}.

The lifetimes of several vibrational levels of the S_1 state of free porphyrin base at 4.2 K vary from 1 to 30 ps (Table 8). Totally symmetrical modes in the frequency range from 150 to 1160 cm^{-1} are characterised by substantial variations of the lifetimes. For the modes with frequencies lying between 1340 and $\sim$1580 cm^{-1}, the lifetimes of vibrational levels were estimated at 1.0 to 1.6 ps irrespective of the vibrational mode symmetry. This is in reasonable agreement with the results of measurements of the lifetimes of vibrational levels of organic molecules obtained by other experimental methods.[116, 117] Note that the rates of vibrational relaxation of most of higher excited states are much lower than those of electronic relaxation (see Tables 2–5).

The S_3 state lifetimes of a tetrabenzoporphyrin derivative [a solution in THF–Et_2O (1 : 1) mixture] determined from hole burning experiments at 4.2 K and estimated from the $S_3 \rightarrow S_0$ fluorescence quantum yield have been compared.[140] As in the preceding case, holes were burnt using photochemically induced tautomeric transformation involving inner hydrogen atoms of porphyrin molecule. The hole halfwidth was found to be 10 cm^{-1} for the $S_3 \leftarrow S_0$ transition (λ_{max} = 434 nm), which corresponded to the S_3 level lifetime, τ_3, of 0.53 ps. The lifetime of the same state estimated from the $S_3 \rightarrow S_0$ fluorescence quantum yield and the ratio of the radiative rate constants for the $S_3 \rightarrow S_0$ and $S_1 \rightarrow S_0$ transitions (these were determined from the absorption spectrum) was 1.2 ps. The discrepancy between the two τ_3 values is not too large; however, it seems to be greater than the experimental error. Position of the S_2 level of the tetrabenzoporphyrin derivative has also been determined.[140] The corresponding band in the absorption spectrum is overlapped with vibronic bands of the $S_1 \leftarrow S_0$ transition. However, hole burning measurements allowed the observation of the 0–0 band of the $S_2 \leftarrow S_0$ transition at 606 nm and estimation of the S_2 state lifetime at 0.38 ps. The lifetime of the vibronic sublevel of the S_1 state with an energy of 1108 cm^{-1} was also determined: the hole halfwidth was found to be 0.18 nm, which corresponded to a vibronic level lifetime of 1.1 ps.

Hole burning technique was used for studying internal conversion in Zn-tetraphenylporphyrin molecules incorporated into polymeric matrices at 4 K.[141] The homogeneous broadening in the Soret band was close to that found in the preceding case [140] (see Table 7). Supersonic jet measurements have led to similar results.[142, 143]

The HESS lifetimes were estimated by the photophysical (optical) hole burning method.[144] Previously,[145] this experimental technique was used in a study on the temperature dependence of phase relaxation of the S_1 state of Zn-porphyrin molecule. To burn holes in the $S_2 \leftarrow S_0$ absorption band of phenanthrene (a solution in isopentene–2-methylpentane mixture at 4.2 K), molecules were excited to a triplet state by irradiating samples by the light of a pulsed dye laser with frequency doubling. Absorption was measured using a high-resolution double monochromator. A phosphoroscope was constructed to provide alternate illumination of a sample placed in a cryostat by the laser light and by the transmitted light of a Xe lamp. The homogeneous halfwidth of hole burnt was found to be 67 cm^{-1}, which corresponded to the $S_2(0)$ state lifetime of phenanthrene, τ_2, of 0.079 ps. The lifetime of the S_2 vibronic state (400 cm^{-1}), also determined by both resonance and off-resonance hole burning techniques, was found to be nearly the same. On the other hand, homogeneous linewidth measurements of isolated phenanthrene molecules in a supersonic jet have led to a value of 0.5 ps for $\tau_2(0)$.[146] The reason for such a large difference between the estimates of the lifetimes of the second excited state of phenanthrene molecules is still to be clarified. Indeed, since fast internal conversion occurs intramolecularly, one would expect similar rates of internal conversion for the molecule in the condensed phase and in the vapour phase. Unfortunately, comparable information on the rate constants for internal conversion from higher excited states in the condensed phase and in supersonic jets for the same molecules is scarce.

Nickel and Wick [147] studied the vibrational structure of the $S_0 - S_2$ absorption band of coronene in poly(methyl methacrylate) at 1.8 K by the photophysical hole burning technique. The lifetime of the vibronic S_2 states, estimated from the homogeneous width of resonance transitions, was found to be somewhat shorter than 2 ps. This is in reasonable agreement with the results obtained by different authors [148, 149] who observed fluorescence from the S_2 state of coronene under conditions of direct single-quantum excitation and with the results of measurements of the homogeneous width of fluorescence excitation lines in the Shpolskii matrices and in a supersonic jet. Such a relatively long lifetime of the S_2 state [with the energy gap $\Delta E(S_2 - S_1) \simeq 5000$ cm^{-1}] seems to be due to high molecular symmetry and forbiddenness of the $S_2(^1B_{1u}) \rightarrow S_1(^1B_{2u})$ radiative transitions. Unlike phenanthrene, the homogeneous linewidth of coronene is nearly the same both in a supersonic jet and in the low-temperature matrix.

A large body of information on the linewidths in the molecular spectra (including those of porphyrins) obtained in supersonic jet studies has been reported.[142, 143, 146]

Table 8. Lifetimes of vibrational levels of the S_1 state of free base porphyrin molecules (a solution in n-octane) at 4.2 K.[139]

ν /cm^{-1}	Mode symmetry	Homogeneous width /GHz	τ /ps
0 [a]	A_g	0.017	9.4×10^3
155	A_g	82	1.9
307	A_g	50	3.2
710	A_g	5	32
783	B_{1g}	44	3.6
943	A_g	96	1.7
970	B_{1g}	103	1.5
1161	A_g	5.4	30
1340	A_g	150	1.0
1355	B_{1g}	120	1.3
1583	A_g	100	1.6

[a] The 0–0 transition.

VII. Lifetimes of higher excited S_n states estimated from picosecond and femtosecond spectroscopy data

In the last decade, direct measurements of the HESS lifetimes of organic molecules were reported. To measure the decay of very weak emission from these states with femtosecond resolution is a complicated problem. Conventional experimental techniques involve consecutive stepwise excitation by two picosecond or femtosecond light pulses with a small pulse delay. The second pulse is used for measuring the kinetics of either the induced absorption spectrum or the absorption spectrum reconstruction for the lower-lying state (laser photolysis with picosecond or femtosecond resolution). Excitation by the second pulse also allows photoionisation of a molecule followed by mass-spectrometric or another type of detection of the cation formed or electron detached. Recently, a large number of studies concerning measurements of ultrafast luminescence decay kinetics by luminescence up-conversion, *i.e.*, 'mixing' of weak luminescence with an optically delayed femtosecond pulse in a nonlinear crystal, were reported.

When comparing different methods for studying the dynamics of internal conversion from HESS, preference should be given to those which allow the observation of fluorescence kinetics due to transition from these states. Studies of molecular absorption spectra induced by laser pulses are complicated by three factors, *viz.*, transition-state absorption, ground-state 'bleaching' and stimulated emission from the excited state. The results of second-pulse induced photoionisation studies are also ambiguous.

A stepwise photoionisation study of the lifetime of the S_2 state (35 900 cm^{-1}) of naphthalene in a supersonic jet has been reported.[150] However, only the upper bound of the lifetime of this state (10^{-11} s) was estimated due to instrumental limitations on the pulse duration (6 ps). Quenching of the S_2 fluorescence of Zn(TPP) in acetonitrile due to the addition of dichloromethane has been studied by an up-conversion technique.[151] The lifetime $\tau(S_2)$ of ZnTPP was found to be 3.5 (in acetonitrile) and 0.75 ps (in dichloromethane). Since the S_2 state lifetime is very short, the concentration dependence of fluorescence quenching can be described using the Perrin model:

$$\ln\frac{I_0}{I} = VN_A[CH_2Cl_2],$$

where I_0 is the radiation intensity without a quencher, I is the radiation intensity, $V = (4/3)\pi R^3$ is the action range of the quencher ($R = 15$ Å) and N_A is the Avogadro constant. It was found [151] that quenching of fluorescence from the S_1 state of Zn(TPP) with dichloromethane is inefficient. The authors suggested that quenching of the S_2 fluorescence is due to electron transfer.

Internal conversion in complexes of Zn-porphyrin (ZnP) derivatives and free porphyrin base (H_2P) dissolved in benzene has been studied by femtosecond fluorescence spectroscopy.[152] For ZnP, two fast components of the $S_2(B) \rightarrow S_0$ fluorescence decay were associated with the $S_2 \rightarrow S_1$ internal conversion with a time constant of 150 fs (spectral changes in the region of the $S_2 \rightarrow S_0$ transition) and with vibrational relaxation to the $S_1(Q)$ state with a time constant of 600 fs (spectral changes in the region of the $S_1 \rightarrow S_0$ transition). Free porphyrin base exhibits ultrafast relaxation of the $S_3(B)$ state ($\tau < 40$ fs), fast relaxation of the $S_2(Q_y)$ state with a time constant of 90 fs and a slower vibrational relaxation of the $S_1(Q_x)$ state. A fluorescence up-conversion study of fluorescence decay from the $S_3(^1B_b)$ state of tetracene in solution using 280 fs pulses was carried out.[153] The decay time, τ, of the ($S_3 \rightarrow S_0$) fluorescence of tetracene in the UV region was estimated to be $\sim$120 fs. Usual fluorescence from the $S_1(^1L_a)$ level was found to arise with the same rate constant.

Decay kinetics of the S_2 and S_1 states of Malachite Green dye in different solvents (methanol, water, ethylene glycol and water–glycerol mixture) has been studied by femtosecond fluorescence up-conversion spectroscopy (pulse separation $\Delta t = 90$ fs).[154] The decay times in an aqueous solution were estimated at 0.27 ps for $\tau(S_2)$ and at 0.54 ps for $\tau(S_1)$. If the molecule is excited to the second singlet state, the rise of the S_1 fluorescence and the decay of the S_2 fluorescence occur with the same rate constant.

Femtosecond time-resolved photoelectron spectroscopy ($\Delta t < 200$ fs, $\lambda = 252$ nm) was used for studying ultrafast internal conversion in 1,3,5-hexatriene, which is one of the simplest representatives of polyenes.[155] The S_1 state lifetimes were estimated at 730 and 270 fs for *cis*- and *trans*-hexatriene, respectively. The authors of this study suggested that relaxation process occurs as a cascade, *viz.*, $S_2 \rightsquigarrow S_1 \rightsquigarrow S_0$. The estimate of the S_2 state lifetime, $\tau(S_2) \leqslant 50$ fs, is consistent with that obtained earlier [156] from the homogeneous width of the $S_2 \leftarrow S_0$ absorption line at 250 nm in supersonic jets. The S_2 state decay times were estimated at 50 fs for *trans*-hexatriene and at 20 fs for *cis*-hexatriene. This is close to the S_2 state lifetime of *trans*-hexatriene vapours (40 fs) obtained from the data on resonant Raman scattering.[157]

Femtosecond up-conversion studies of the effect of molecular structure and solvent on the S_2 state lifetimes of carotenoids have been reported.[158, 159] They revealed violation of Kasha's rule [8] and Ermolaev–Sveshnikova's rule [160, 161] (the sum of the fluorescence and triplet-state generation quantum yields equals unity for solutions of fluorescent compounds) in the case of linear polyenes including carotenoids. It was pointed also out that the main emission of molecules with C_{2h} symmetry originates from the S_2 level (the $S_2 \rightarrow S_1$ radiative transition is forbidden). If the molecular symmetry is broken, the S_1 emission becomes stronger. The τ_2 values for the three compounds studied lie between 100 and 200 fs. More recently, in studies of neurosporene (a linear carotenoid) it has been shown [162] that excitation to the S_2 state with an excess vibrational energy of $\sim$3000 cm^{-1} leads to the appearance of a time-dependent $S_2 \rightarrow S_0$ fluorescence spectrum. This was explained by the vibrational energy redistribution in the S_2 state from the Franck–Condon active modes to other (dark) modes with a time constant of 35–40 fs, followed by the $S_2 \rightarrow S_1$ internal conversion occurring in 250 fs.

The effect of hydrogen bond formation/dissociation on the relaxation rate of the S_3 and S_2 states of *trans*-retinal molecules (a solution in butan-1-ol–cyclohexane mixture) on the subpicosecond time scale has been first studied recently.[163] The $S_3[B_u^+(\pi,\pi^*)]$ and $S_2[A_g^-(\pi,\pi^*]$ state lifetimes of the molecules under study in neat butan-1-ol (200 fs and 1.8 ps, respectively) were found to be much longer than the corresponding lifetimes in neat cyclohexane (30 fs and 0.7 ps, respectively). In the S_2 state, all the *trans*-retinal molecules are hydrogen-bonded. The increase in the fluorescence and the isomerisation quantum yields and the decrease in the triplet quantum yield upon hydrogen bond formation were explained by the prolonged lifetime of the S_2 state of *trans*-retinal. The authors cited were the first to study the formation and cleavage of a hydrogen bond in a subpicosecond time.

Hirata *et al.*[164, 165] studied the dependence of the rate constant for the $S_2 \rightarrow S_1$ internal conversion on the energy gap width in the molecules of (i) diphenylacetylene and its derivatives and (ii) *trans*-α,ω-diphenylpolyenes with different chain length (solutions in n-hexane and THF were used in both cases). The S_2 state lifetimes of diphenylpolyenes with the molecular chains of length from 3 to 8 monomer units and the energy gaps of width from 1600 to 4800 cm^{-1} varied insignificantly (500 ± 100 fs) and increased only slightly with the decrease in the temperature. The rate constant for the $S_1 \rightarrow S_0$ nonradiative transition increased by three orders of magnitude for the same diphenylpolyenes.

A femtosecond laser flash photolysis study on fast photo-induced reactions of *trans*-azobenzene excited to the S_2 state (in solutions at 303 K, $\sim$200 fs resolution) has been reported.[166] Analysis of the induced absorption decay curve measured in the region 370–450 nm revealed its two-exponential structure and

allowed determination of the time constants which appeared to be different for different solvents. The time constant for the fast exponent, τ_1, was found to be 0.9 ps for hexane, cyclohexane and hexadecane and 1.2 ps for acetonitrile. That for the slow exponent, τ_2, was found to be 13 ps for the hydrocarbons and 16 ps for acetonitrile. The authors suggested that the decay of the fast exponent is due to deactivation of the $S_2(\pi,\pi^*)$ state. The appearance of the slow exponent was explained by the presence of an intermediate excited singlet state lying between the S_2 and S_1 states on the energy scale, corresponding to the *twist*-conformer of the excited *trans*-azobenzene molecule. The dynamics of the S_2 and S_1 states of *trans*-4-n-butyl-4′-methoxyazabenzene in hexane has been studied [167] by a similar experimental technique with the same resolution. The time constants were estimated at $\approx$250 fs for $\tau(S_2)$ and at 2.3 ps for $\tau(S_1)$.

Femtosecond time-resolved photoelectron spectroscopy was used for measuring the S_n state lifetimes of pyrazine molecules in a supersonic jet.[168] In particular, the lifetime of the S_2 state, $\tau(S_2)$, was estimated at 20 fs. A supersonic jet study of the S_2 state of benzene – ammonia complexes has been reported.[169] The S_2 state lifetime was estimated at $\sim$100 fs.

Fluorescence of coumarin 481 in cyclohexane at 293 K, which appeared after excitation by 100 fs pulses at $\lambda = 267$ nm has been studied in detail.[170] The molecules were excited to an S_n state lying 12 000 cm^{-1} higher than the S_1 state and then the dynamics of the rise of the $S_1 \rightarrow S_0$ fluorescence was observed using up-conversion technique. The time constant of the rise of the fluorescence in the region 419 – 475 nm was found to be 280 to 220 fs. This time was interpreted as that required for completion of the $S_n \rightarrow S_1$ internal conversion. It was also suggested that intramolecular redistribution of vibrational energy in the S_1 and S_0 states occurs with strongly different rates.[170]

However, there is also another concept of the redistribution of excess vibrational energy in the ground and first excited states after optical excitation.[20] The authors came to conclusion that vibrational excitation is redistributed in the S_0 and S_1 states of dye molecules with the same rate constant. Based on analysis of their original studies and published data, they also suggested that in most cases redistribution of excess vibrational energy involves two stages. The first stage is fast, with a time constant τ_1 estimated at 30 to 200 fs, while the second stage is slow, with a time constant τ_2 estimated at 200 to 1000 fs. It was assumed that the fast stage is due to the interaction of isoenergetic vibrational levels, whereas the slow stage is due to coupling of levels with different energies. Yet another assumption is that the time required to 'cool' a vibrationally 'overheated' molecule *via* transfer of excess energy to the environment (solvent molecules) should be much longer (from 15 to 40 ps for different solvents).

The dynamics of IR 125 dye in ethylene glycol solution was studied by pump-probe experiments.[171, 172] The pump pulse duration was 30 fs ($\lambda = 425$ nm) while the probe pulse width was 20 fs ($\lambda = 850$ nm). It was found that a dye molecule excited to an S_n ($n > 1$) state by a pulse at $\lambda = 425$ nm arrives at the S_1 state within 50 fs; however, the time constant of S_1 population (accumulation of molecules at the minimum of the PES of this state) is much larger ($\sim$1 ps).

A number of papers concerning nonradiative transitions between higher excited electronic levels of the molecules comprised of ten or smaller number of atoms was reported. In particular, the S_2 state lifetimes of acetone and its deuterated analogue in the vapour phase were studied using femtosecond photoionisation ($\lambda_{exc} = 194$ nm, $\lambda_{ion} = 295$ nm).[173] It was found that $\tau(S_2) = 13.5$ ps for acetone-d_6 and 4.7 ps for acetone-h_6. In this case, the S_1 state lifetimes of both molecules (< 150 fs) are shorter than the corresponding S_2 state lifetimes. This is similar to azulene and β-carotenes.

VIII. Ultrafast nonradiative transitions involving triplet states

A salient feature of aromatic and dye molecules is the possibility of ultrafast nonradiative transitions involving triplet states. Naturally, the question arises of the rates of such transitions.

Liu and Edman [174] studied photoisomerisation reactions of various alkenes sensitised by anthracene and its derivatives. All the reaction pathways were known to pass through triplet states. The authors assumed that the photoreactions can proceed only *via* excited molecules of anthracene and its derivatives. Since the lowest triplet levels of anthracenes lie much below those of alkenes, it was suggested that the reactions under study proceed due to energy transfer from the second triplet level (T_2) of the anthracenes and that the T_2 level is populated *via* intersystem crossing from the S_1 state. [The T_2 level of the sensitiser molecules lies somewhat lower than their first excited singlet level, $E(T_2) = 25\,000 - 26\,000$ cm^{-1}]. Among all the alkene reactions studied, the highest quantum yield (0.042) was found for *cis – trans* isomerisation of piperylene in benzene (0.2 M) at 293 K sensitised by 9,10-dibromoanthracene. Assuming that the rate constant for triplet – triplet energy transfer from the T_2 level is equal to the diffusion rate constant, the T_2 state lifetime of 9,10-dibromoanthracene was estimated at 1.3×10^{-10} s.[175]

An alternative explanation for the results obtained by Liu and Gale [175] has been put forward in a paper [176] concerning fluorescence quenching of haloanthracenes by naphthalene and phenanthrene. Taking into account a correlation between the rate constants for quenching and the spin-orbit coupling constants of anthracene derivatives, the authors concluded that a spin-forbidden, singlet – triplet energy transfer occurs in this case. Similarly to the earlier results,[175] the most pronounced effect was observed for 9,10-dibromoanthracene. It was also assumed [176] that this process should also lead to population of triplet states of the energy acceptor and can induce alkene isomerisation.

Only a few observations of the fluorescence due to triplet – triplet transitions have been reported. For instance, $T_2 - T_1$ fluorescence was detected upon excitation of certain anthracene derivatives dissolved in methylcyclohexane to the S_1 state.[80, 177] Fluorescence spectra were measured in air at room temperature. The 0 – 0 bands in the $T_2 - T_1$ fluorescence spectra of these compounds lie in the region from 840 to 960 nm (12 000 – 10 400 cm^{-1}) and are nearly mirror images of the long-wavelength $T_n \leftarrow T_1$ absorption bands. The $T_2 \rightarrow T_1$ fluorescence quantum yields were estimated at 10^{-6} for 9,10-dibromoanthracene [$\tau(T_2) = 2 \times 10^{-12}$ s] and at 5×10^{-8} for the unsubstituted anthracene [$\tau(T_2) = 10^{-13}$ s]. These values are in poor agreement with indirect estimates of the T_2 state lifetime of anthracene, obtained from the results of photochemical sensitisation studies.[178]

Keller [179] was the first to report on the reverse intersystem crossing from higher excited triplet states of aromatic molecules to the excited singlet levels. At 77 K, aromatic molecules in a glassy matrix were excited by UV irradiation to populate the lowest triplet state. Then the molecules were excited by visible light into the $T_n \leftarrow T_1$ absorption bands and their UV fluorescence accompanying the $S_1 \rightarrow S_0$ transition (Fig. 9) was observed. The fluorescence intensity was proportional to the intensity of visible light and the fluorescence lifetime was identical to the lifetime of the lowest triplet T_1 state. The quantum yield of the triplet – singlet intersystem crossing process (the ratio of the number of $T_n \rightarrow S_1$ transitions to the number of photons absorbed by the T_1 state) is small, namely, 5×10^{-7} for naphthalene, 2×10^{-6} for quinoline and 10^{-6} for fluorene. Kobayashi *et al.*[180] also observed the $S_1 \rightarrow S_0$ fluorescence of anthracene and its 9-methyl and 9-phenyl derivatives due to reverse intersystem crossing. The quantum yield of the $T_n \rightarrow S_1$ intersystem crossing was estimated at 5×10^{-6} for anthracene and at 8×10^{-5} for 9-phenylanthracene. More recently [181] some arguments were adduced in favour of assumption that the S_1 state of 9,10-dibromoanthracene molecule is

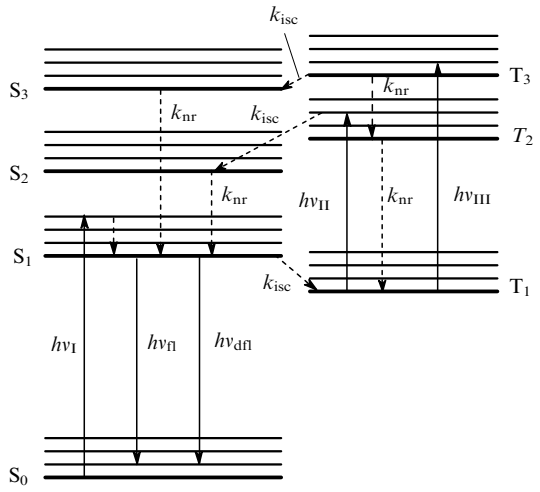


Figure 9. An energy level diagram illustrating the appearance of delayed fluorescence (ν_{dfl}) after excitation of a molecule to a higher excited triplet state and intersystem crossing from this state to the singlet manifold.

populated *via* absorption of a light quantum by the T_1 state and is also due to the $S_m \leftarrow T_1$ transition. Population of the fluorescent state of perylene vapours *via* excitation of the lowest triplet state by consecutive irradiation by two laser pulses has been reported.[182]

A version of Keller's technique [179] which uses stepwise excitation by nanosecond laser pulses has been proposed in studies of xanthene dyes (eosin, erythrosin and Rose Bengal) in polymeric matrices.[183, 184] The authors simultaneously observed both the delayed fluorescence induced by the second delayed pulse and the decrease in the optical density of the triplet–triplet absorption, which was rationalised by the occurrence of the $T_n \rightarrow S_m$ reverse intersystem crossing. Thus, a competition of nonradiative intersystem crossing with internal conversion over the triplet manifold is implied. This is quite probable since the molecules studied contain heavy Br or I atoms. However, too high quantum yields of the process [183, 184] are suspicious because the spin-forbidden transition competes with the spin-allowed process of internal conversion over the triplet manifold.

Similar approach was used in studies of the $S_1 \rightarrow S_0$ fluorescence of Rose Bengal in aqueous solutions (a phosphate buffer, pH 7.0).[185] Fluorescence appeared after stepwise excitation of the dye molecules from the lowest triplet state to excited triplet states, followed by reverse intersystem crossing to the singlet manifold and emission. An intense absorption band at $\lambda_{max} = 1063$ nm was detected by near-infrared laser flash photolysis measurements and assigned to the $T_2 \leftarrow T_1$ transition.[185] It was found that excitation of the dye by the second harmonic of a Nd laser ($\lambda = 532$ nm, $t_{pulse} = 134$ ps) to the S_1 state leads to population of the T_1 triplet state with a probability of 0.98 and to fluorescence emission with a quantum yield of 0.02. The second pulse of the fundamental frequency of the Nd laser excited the solution with a delay of 34 ns to populate the T_2 state since the fundamental frequency of neodymium penetrates the long-wavelength triplet–triplet absorption band.

Population of the T_3 state was achieved by irradiating the solution by the second pulse ($\lambda = 632$ nm) with the same delay. Then, the dependence of the intensity of two-step, laser-induced delayed fluorescence on the intensity of laser pulses was measured and analysis using a simplified kinetic scheme was performed. As a result, the quantum yield of the $T_2 \rightarrow S_1$ reverse intersystem crossing, $q(T_2,S_1)$, was estimated at 0.014 and the T_2 state lifetime, $\tau(T_2)$, was found to be 5.8 ps.[185] No $S_1 \rightarrow S_0$ fluorescence was observed upon two-step laser-induced excitation at $\lambda_2 = 632$ nm *via* the T_1 state. Therefore, only the upper bound of the reverse intersystem crossing yield from the T_3 state, $q(T_3 \rightarrow S_n)$, was estimated at 0.06. These results strongly disagree with those obtained in earlier studies,[183, 184], according to which $q(T_3 \rightarrow S_n) = 0.74$. Previously,[183] this value was estimated from the decrease in the T_1 state population of the dye after irradiation by the second pulse at $\lambda_2 = 632$ nm.

Table 9. Quantum yields of reverse intersystem crossing for excited triplet levels of Rose Bengal dye molecule.[185]

Energy level	E /cm^{-1}	$\Delta E(T_n \rightarrow S_n)$ /cm^{-1}	$\Delta E(T_n \rightarrow T_{n-1})$ /cm^{-1}	$q(T_n \rightarrow S_n)$
T_2	23 550	4030	9435	0.014
T_3	31 130	2820	7580	< 0.06
T_4	32 500	640	1370	0.8

Previously (see, *e.g.*, Refs 186 and 187), it was assumed that the reverse intersystem crossing occurs mainly from the T_2 level. However, the results of measurements of the quantum yield $q(T_n \rightarrow S_n)$ for Rose Bengal rule out this assumption. Table 9 lists the quantum yields of reverse intersystem crossing, positions of triplet levels and the energy gaps between them and the nearest lower-energy triplet and singlet levels of the Rose Bengal molecule. As can be seen, the quantum yields of reverse intersystem crossing are satisfactorily described by the 'energy gap law'; however, it should be remembered that internal conversion over the triplet manifold leads to the energy gap narrowing with increase in the level number. This casts some doubts on the too high yield of reverse intersystem crossing from the T_4 level, though the strength of the spin-orbit coupling between particular triplet and singlet states plays a significant role in this case.[185]

It was found that the addition of LiBr in combination with stepwise excitation to HESS leads to an increase in the quantum yield of triplet rhodamine generation in solution.[188]

IX. Conclusion

The results obtained using different methods of determination of the rate constants for ultrafast nonradiative transitions, considered in this review are, with rare exception, in reasonable agreement with one another. Those obtained by recently developed but rather widely used direct picosecond and femtosecond methods for measuring the fluorescence decay have for the most part confirmed indirect estimates based on the fluorescence yields from HESS under conditions of single-quantum or two-quantum excitation to corresponding levels and found from the homogeneous absorption linewidths. It was established that in most cases the HESS lifetimes of organic and dye molecules are of the order of tens of femtoseconds. The only exception is the second excited singlet state (S_2), the lifetime of which for a number of molecules is much longer, so that it can be considered as a specific state similar to the fluorescent state (S_1). More complex is the problem of theoretical interpretation of experimental results. Correspondence between the observed rate constants and predictions of modern theories of nonradiative transitions is fragmentary. In some instances even the 'physical' or 'chemical' mechanism responsible for the nonradiative transition remains unclear. Undoubtedly, the development of femtosecond measuring devices will provide the possibility of obtaining new information on transitions between HESS. For instance, only in the very recent past has it been possible to observe non-exponential fluorescence decay due to transitions from the HESS, which is interpreted as superimposed 'hot' fluorescence.

'Physical' ultrafast nonradiative transitions can occur by tunneling and as conical intersections of the PES of excited states. Comprehensive theory of nonradiative transitions, based on calculations of possible fast processes due to such conical intersections in complex molecules is now at an early stage. The state-of-the-art in multidimensional theory of nonadiabatic transitions

in the case of conical intersections of the PES has been recently considered in a special issue of the *Chemical Physics* journal.[189]

The author expresses his gratitude to Dr. B Nickel for submitting materials and valuable discussions and to Prof. V A Benderskii for valuable critical comments. This review has been written with the financial support of the Russian Foundation for Basic Research (Project No. 00-03-32208) and the Ministry of Industry, Science and Technology of the Russian Federation.

References

1. A L Buchachenko *Usp. Khim.* **68** 99 (1999) [*Russ. Chem. Rev.* **68** 85 (1999)]
2. A H Zewail *Femtochemistry: Ultrafast Dynamics of the Chemical Bond* (Singapore: World Sci., 1994)
3. V Sundstrom (Ed.) *Femtochemistry and Femtobiology* (Singapore: World Sci., 1998)
4. S I Vavilov*Philos. Mag.* **43** 307 (1922)
5. S I Wawilow *Z. Phys.* **42** 311 (1927)
6. A N Terenin *Acta Phys. Chim. USSR* **18** 210 (1943)
7. G Lewis, M Kasha *J. Am. Chem. Soc.* **66** 2100 (1944)
8. M Kasha *Discuss. Faraday Soc.* **9** 14 (1950)
9. R Englman *Nonradiactive Decay of Ions and Molecules in Solids* (Amsterdam: North-Holland, 1979)
10. E S Medvedev, V I Osherov *Teoriya Bezyzluchatel'nykh Perekhodov v Mnogoatomnykh Molekulakh* (The Theory of Nonradiate Transitions in Polyatomic Molecules) (Moscow: Nauka, 1983)
11. E S Medvedev, V I Osherov *Radiationless Transition in Polyatomic Molecules (Ser. Chemical Physics)* Vol. 57 (Berlin: Springer, 1995)
12. A Nitzan, J Jortner, P M Rentzepis *Proc. R. Soc. London, A Math. Phys. Sci.* **327** 367 (1972)
13. J Jortner, S A Rice, R M Hochstrasser, in *Advances in Photochemistry* (Eds J N Pitts Jr, G S Hammond, W A Noyes Jr) (New York; London: Wiley, 1969) Vol. 7, p. 149
14. E B Sveshnikova, V L Ermolaev *Opt. Spektrosk.* **30** 379 (1971) [a]
15. E N Bodunov *Opt. Spektrosk.* **40** 942 (1976) [a]
16. V L Ermolaev, E B Sveshnikova, E N Bodunov *Usp. Fiz. Nauk* **166** 279 (1996) [b]
17. V L Ermolaev, E N Bodunov, E B Sveshnikova, T A Shakhverdov *Bezyzluchatel'nyi Perenos Energii Elektronnogo Vozbuzhdeniya* (Nonradiate Transfer of Electronic Excitation Energy) (Leningrad: Nauka, 1977)
18. V L Ermolaev, E B Sveshnikova *Chem. Phys. Lett.* **23** 349 (1973)
19. V L Ermolaev, E B Sveshnikova *Acta Phys. Pol. A* **95** 299 (1999)
20. T Elsaesser, W Kaiser *Annu. Rev. Phys. Chem.* **42** 83 (1991)
21. G B Tolstorozhev, S A Tikhomirov *Zh. Prikl. Spektrosk.* **65** 635 (1998)
22. M Beer, H C Longuet-Higgins *J. Chem. Phys.* **23** 1390 (1955)
23. G Viswanath, M Kasha *J. Chem. Phys.* **24** 574 (1956)
24. B D Wagner, D Tittelbach-Helmrich, R P Steer *J. Phys. Chem.* **96** 7904 (1992)
25. D Huppert, J Jortner, P M Rentzepis *J. Chem. Phys.* **56** 4826 (1972)
26. J B Birks *Photophysics of Aromatic Molecules* (London; New York; Sydney; Toronto: Wiley-Interscience, 1969)
27. P M Rentzepis, J Jortner, R P Jones *Chem. Phys. Lett.* **4** 599 (1970)
28. D Huppert, J Jortner, P M Rentzepis *Chem. Phys. Lett.* **13** 225 (1972)
29. G D Gillispie, E C Lim *J. Chem. Phys.* **65** 4314 (1976)
30. G D Gillispie, E C Lim *J. Chem. Phys.* **68** 4578 (1977)
31. D Klemp, B Nickel *Chem. Phys. Lett.* **130** 493 (1986)
32. Y Hirata, E C Lim *J. Chem. Phys.* **69** 3292 (1978)
33. M Fujii, T Ebata, N Mikami, M Ito *Chem. Phys.* **77** 191 (1983)
34. G Eber, S Schneider, F Dorr *Chem. Phys. Lett.* **52** 59 (1977)
35. S Murata, C Iwanaga, T Toda, H Kokubun *Ber. Bunsenges. Phys. Chem.* **76** 1176 (1972)
36. E P Ippen, C V Shank, R L Woerner *Chem. Phys. Lett.* **46** 20 (1977)
37. C V Shenk, E P Ippen, O Teschke, R L Fork *Chem. Phys. Lett.* **57** 433 (1978)
38. E W-G Diau, S De Feyter, A H Zeweil *J. Chem. Phys.* **110** 9785 (1999)
39. M J Bearpark, F Bernardi, S Clifford, M Olivucci, M A Robb, B R Smith, T Vreven *J. Am. Chem. Soc.* **118** 169 (1996)
40. G Eber, F Gruneis, S Schneider, F Dorr *Chem. Phys. Lett.* **29** 397 (1974)
41. R Klann, R J Bauerle, F Laermer, T Elsaesser, M Niemeyer, W Luttke *Chem. Phys. Lett.* **169** 172 (1990)
42. A Falchi, C Gellini, P R Salvi, K Hafner *J. Phys. Chem. A* **102** 5006 (1998)
43. A Falchi, C Gellini, P R Salvi, K Hafner *J. Phys. Chem. A* **104** 1078 (2000)
44. M J Bearpark, M A Robb *J. Phys. Chem. A* **104** 1075 (2000)
45. U P Wild, H J Griesser, V D Tuan, J F M Oth *Chem. Phys. Lett.* **41** 450 (1976)
46. B Nickel, J Hertzberg *Chem. Phys.* **132** 219 (1989)
47. J R Huber, M Mahaney *Chem. Phys. Lett.* **30** 410 (1975)
48. M H Hui, P de Mayo, R Suan, W R Ware *Chem. Phys. Lett.* **31** 257 (1975)
49. M Mahaney, J R Huber *Chem. Phys.* **9** 371 (1975)
50. A Maciejewski, R P Steer *J. Am. Chem. Soc.* **105** 6738 (1983)
51. A Maciejewski, R P Steer *Chem. Rev.* **93** 67 (1993)
52. A Maciejewski, R P Steer *J. Phys. Chem.* **92** 6939 (1988)
53. M Szymanski, R P Steer *J. Phys. Chem.* **96** 8719 (1992)
54. M Szymanski, A Maciejewski, J Kozlowski, J Koput *J. Phys. Chem. A* **102** 677 (1998)
55. H Eisenberger, B Nickel *J. Chem. Soc., Faraday Trans.* **92** 733 (1996)
56. H Eisenberger, B Nickel, A A Ruth, R P Steer *J. Chem. Soc., Faraday Trans.* **92** 741 (1996)
57. B Nickel, H Eisenberger, M T Wick, R P Steer *J. Chem. Soc., Faraday Trans.* **92** 1101 (1996)
58. M Szimanski, A Maciejewski, R P Steer *J. Phys. Chem.* **92** 2485 (1988)
59. M Szimanski, A Maciejewski, R P Steer *J. Photochem. Photobiol. A* **57** 405 (1991)
60. A Maciejewski, M Milewski, M Szimanski *J. Chem. Phys.* **111** 8462 (1999)
61. B Nickel *J. Lumin.* **44** 1 (1989)
62. J Cai, E C Lim *J. Chem. Phys.* **95** 3014 (1991)
63. L Bajema, M Gouterman, C B Rose *J. Mol. Spectrosc.* **39** 421 (1971)
64. I E Zalesskii, V N Kotlo, A N Sevchenko, K N Solov'ev, S F Shkirman *Dokl. Akad. Nauk SSSR* **210** 312 (1973) [c]
65. V N Kotlo, K N Solov'ev, S F Shkirman *Izv. Akad. Nauk SSSR, Ser. Fiz.* **39** 1972 (1975)
66. A V Nikolaitchik, M A J Rodgers *J. Phys. Chem. A* **103** 7597 (1999)
67. L A Martarano, Ch-P Wong, W DeW Horrocks Jr, A M Goncalves *J. Phys. Chem.* **80** 2389 (1976)
68. Y Kurabayashi, K Kikuchi, H Kokubun, Y Kaizu, H Kobayashi *J. Phys. Chem.* **88** 1308 (1984)
69. M P Tsvirko, G F Stelmakh, V E Pyatosin, K N Solovyov, T F Kachura *Chem. Phys. Lett.* **73** 80 (1980)
70. V L Ermolaev, I P Kotlyar, V A Lyubimtsev, V G Maslov *Opt. Spektrosk.* **52** 3 (1982) [a]
71. N Mataga, Y Shibata, H Chosrowjan, N Yoshida, A Osuka *J. Phys. Chem. B* **104** 4001 (2000)
72. V L Ermolaev, V A Lyubimtsev *Tr. Gos. Opt. Inst. im. S I Vavilova* **65** (199) 20 (1987)
73. A Janovski, J Rzeszotarska *J. Lumin.* **21** 409 (1980)
74. M Yoshizawa, K Suzuki, A Kubo, S Saikan *Chem. Phys. Lett.* **290** 43 (1998)
75. T A Gregory, S Lipsky *J. Chem. Phys.* **65** 296 (1976)
76. F Hirayma, T A Gregory, S Lipsky *J. Chem. Phys.* **58** 4696 (1973)
77. T A Gregory, F Hirayma, S Lipsky *J. Chem. Phys.* **58** 4697 (1973)
78. P O Andersson, S M Bachilo, R-L Chen, T Gillbro *J. Phys. Chem.* **99** 16199 (1995)
79. R Katoh, S Fujiyoshi, M Kotani *Chem. Phys. Lett.* **292** 621 (1998)
80. G D Gillispie, E C Lim *J. Chem. Phys.* **65** 2022 (1976)
81. L A Hallidy, M R Topp *Chem. Phys. Lett.* **46** 8 (1977)
82. A Terenin, G Kobyshev, G Lialin *Photochem. Photobiol.* **5** 689 (1966)
83. W E Gibbs *Appl. Phys. Lett.* **11** 113 (1967)
84. A Muller, E Pfluger *Chem. Phys. Lett.* **2** 155 (1968)
85. M D Galanin, Z A Chizhikova *Kratkie Soobshch. po Fizike* (4) 35 (1971)
86. M D Galanin, Z A Chizhikova *Izv. Akad. Nauk SSSR, Ser. Fiz.* **36** 941 (1972)
87. E N Kaliteevskaya, T K Razumova *Opt. Spektrosk.* **36** 1118 (1974) [a]
88. D Leupold, R Konig, B Voigt *J. Lumin.* **9** 113 (1974)
89. V Rehak, A Novak, M Titz *Chem. Phys. Lett.* **52** 39 (1974)
90. G C Orner, M R Topp *Chem. Phys. Lett.* **36** 295 (1975)
91. H-B Lin, M R Topp *Chem. Phys. Lett.* **47** 442 (1977)
92. H-B Lin, M R Topp *Chem. Phys. Lett.* **48** 251 (1977)

93. M R Topp, H-B Lin *Chem. Phys. Lett.* **50** 412 (1977)
94. H-B Lin, M R Topp *Chem. Phys. Lett.* **67** 273 (1979)
95. M R Topp, H-B Lin, K-J Choi *Chem. Phys.* **60** 47 (1981)
96. B Nickel, G Roden *Ber. Bunsenges. Phys. Chem.* **81** 281 (1977)
97. V A Lyubimtsev, Candidate Thesis in Physicomathematical Sciences, Leningrad State University, Leningrad, 1989
98. R I Personov, E I Al'shits, L A Bykovskaya *Opt. Commun.* **6** 169 (1972)
99. B M Kharlamov, R I Personov, L A Bykovskaya *Opt. Commun.* **12** 191 (1974)
100. V L Ermolaev, V A Lyubimtsev *Izv. Akad. Nauk SSSR, Ser. Fiz.* **47** 1405 (1983)
101. V L Ermolaev, V A Lyubimtsev *Opt. Spektrosk.* **56** 1026 (1984) [a]
102. V L Ermolaev, V A Lyubimtsev *Opt. Spektrosk.* **60** 74 (1986) [a]
103. V L Ermolaev, V A Lyubimtsev *Opt. Spektrosk.* **60** 970 (1986) [a]
104. V A Lyubimtsev, V L Ermolaev *Opt. Spektrosk.* **61** 511 (1986) [a]
105. V A Lyubimtsev, V L Ermolaev *Opt. Spektrosk.* **61** 766 (1986) [a]
106. V L Ermolaev, V A Lubimtsev *Acta Phys. Pol. A* **71** 731 (1987)
107. A A Krasheninnikov, A V Shablya *Opt. Spektrosk.* **60** 70 (1986) [a]
108. V P Klochkov, V L Bogdanov *Zh. Prikl. Spektrosk.* **43** 5 (1985)
109. R I Personov, E I Al'shits, L A Bykovskaya *Pis'ma Zh. Eksp. Teor. Fiz.* **15** 609 (1972)
110. A P Veduta, M D Galanin, B P Kirsanov, Z A Chizhikova *Pis'ma Zh. Eksp. Teor. Fiz.* **11** 157 (1970)
111. V L Bogdanov, in *Topics in Fluorescence Spectroscopy. Nonlinear and Two-Photon-Induced Fluorescence* (Ed. J R Lakowicz) (New York; London: Plenum, 1997) Vol. 5, p. 211
112. V L Bogdanov, V P Klochkov *Opt. Spektrosk.* **48** 34 (1980) [a]
113. V A Lyubimtsev *Izv. Akad. Nauk SSSR, Ser. Fiz.* **54** 391 (1990)
114. T P Kravets *Izv. Mosk. Inzh. Uchil., Ser. 2* (6) (1912)
115. S J Strickler, R A Berg *J. Am. Chem. Soc.* **37** 814 (1962)
116. N M Cottfried, A Seilmeier, W Kaiser *Chem. Phys. Lett.* **111** 326 (1984)
117. J Scherer, A Seilmeier, W Kaiser *J. Chem. Phys.* **83** 3948 (1985)
118. J L Baudour, H Caillean, W B Yelon *Acta Crystallogr., Sect. B, Struct. Crystallogr.* **33** 1773 (1977)
119. G V Maier, V P Shcherbina *Opt. Spektrosk.* **52** 1063 (1982) [a]
120. B Nickel *Chem. Phys. Lett.* **27** 84 (1974)
121. B Nickel *Helv. Chim. Acta* **61** 198 (1978)
122. B Nickel *Chem. Phys. Lett.* **71** 238 (1980)
123. B Nickel, G Roden *Chem. Phys.* **53** 243 (1980)
124. B Nickel, G Roden *Chem. Phys. Lett.* **74** 368 (1980)
125. G F Stel'makh, M P Tsvirko *Opt. Spektrosk.* **50** 998 (1981)
126. B Nickel *Chem. Phys. Lett.* **68** 17 (1979)
127. Y J Kray, B Nickel *Chem. Phys.* **53** 235 (1980)
128. D Klemp, B Nickel *Chem. Phys. Lett.* **97** 66 (1983)
129. B Nickel, G Roden *Chem. Phys.* **66** 365 (1982)
130. J Hertzberg, B Nickel *Chem. Phys.* **132** 235 (1989)
131. D L Dexter *J. Chem. Phys.* **21** 836 (1953)
132. R Katoh, M Kotani *Chem. Phys. Lett.* **201** 141 (1993)
133. R Katoh, M Kotani *Chem. Phys. Lett.* **300** 734 (1999)
134. R M Hochstrasser, C Marzzacco *J. Chem. Phys.* **49** 971 (1968)
135. J L Richards, S A Rice *Chem. Phys. Lett.* **9** 444 (1971)
136. S Voelker, J H van der Waals *Mol. Phys.* **32** 1703 (1976)
137. S Voelker, R M Macfarlane, A Z Genack, H P Trommsdorff, J H van der Waals *J. Chem. Phys.* **67** 1759 (1977)
138. S Voelker, R M Macfarlane, J H van der Waals *Chem. Phys. Lett.* **53** 8 (1978)
139. S Voelker, R M Macfarlane *Chem. Phys. Lett.* **61** 421 (1979)
140. V G Maslov *Opt. Spektrosk.* **50** 1091 (1981) [a]
141. M Vacha, Sh Machida, K Horie *J. Phys. Chem.* **99** 13163 (1995)
142. U Even, J Jortner, J Friedman *J. Phys. Chem.* **86** 2273 (1982)
143. U Even, J Magen, J Jortner *J. Chem. Phys.* **77** 4384 (1982)
144. B Dick, B Nickel *Chem. Phys.* **110** 131 (1986)
145. R M Shelby, R M Macfarlane *Chem. Phys. Lett.* **64** 545 (1979)
146. A Amirav, M Sonnenschein, J Jortner *J. Phys. Chem.* **88** 5593 (1984)
147. B Nickel, M T Wick *Chem. Phys.* **168** 111 (1992)
148. C-J Ho, J Babbitt, M R Topp *J. Phys. Chem.* **91** 5599 (1987)
149. R Jefferson, J Babbitt, C-J Ho, M R Topp *J. Phys. Chem.* **92** 2422 (1988)
150. A Hiraya, Y Achiba, N Mikami, K Kimura *J. Chem. Phys.* **82** 1810 (1985)
151. H Chosrowjan, S Tanigichi, T Okada, S Takagi, T Arai, K Tokumaru *Chem. Phys. Lett.* **242** 644 (1995)
152. S Akimoto, T Yamazaki, I Yamazaki, A Osuka *Chem. Phys. Lett.* **309** 177 (1999)
153. N Sarkar, S Takeuchi, T Tahara *J. Phys. Chem. A* **103** 4808 (1999)
154. C C Hayden, D W Chandler *J. Phys. Chem.* **99** 7897 (1995)
155. D R Cyr, C C Hayden *J. Chem. Phys.* **104** 771 (1996)
156. D G Leopold, R D Pandley, J L Roebber, R J Hemley, V Vaida *J. Chem. Phys.* **81** 4218 (1984)
157. A B Myers, K S Pranata *J. Phys. Chem.* **93** 5079 (1989)
158. M Mimuro, U Nagashima, S Nagaoka, S Takaichi, I Yamazaki, Y Nishimura, T Katoh *Chem. Phys. Lett.* **204** 101 (1993)
159. M Mimuro, S Akimoto, S Takaichi, I Yamazaki *J. Am. Chem. Soc.* **119** 1452 (1997)
160. V L Ermolaev *Usp. Fiz. Nauk* **80** 3 (1963) [b]
161. V L Ermolaev, E B Sveshnikova *Acta Phys. Pol.* **34** 771 (1968)
162. S Akimoto, I Yamazaki, S Takaichi, M Mimuro *Chem. Phys. Lett.* **313** 63 (1999)
163. Sh Yamaguchi, H Hamaguchi *J. Phys. Chem. A* **104** 4272 (2000)
164. Y Hirata, T Okada, N Mataga, T Nomoto *J. Phys. Chem.* **96** 6559 (1992)
165. Y Hirata, K Mashima, H Fukumoto, K Tani, T Okada *Chem. Phys. Lett.* **308** 176 (1999)
166. I K Lednev, N-Q Ye, R E Hester, J N Moore *J. Phys. Chem.* **100** 13338 (1996)
167. J Azuma, N Tamai, A Shishido, T Ikeda *Chem. Phys. Lett.* **288** 77 (1998)
168. V Stern, P Farmanara, W Radloff *J. Chem. Phys.* **112** 4460 (2000)
169. W Radloff, Th Freudenberg, H-H Ritze, V Stern, K Weyers, F Noack *Chem. Phys. Lett.* **245** 400 (1995)
170. K Ohta, T J Kang, K Tominaga, K Yoshihara *Chem. Phys.* **242** 103 (1999)
171. T Hasche, S H Ashworth, E Riedle, M Woerner, T Elsaesser *Chem. Phys. Lett.* **244** 164 (1995)
172. S H Ashworth, T Hasche, M Woerner, E Riedle, T Elsaesser *J. Chem. Phys.* **104** 5761 (1996)
173. J C Owrutsky, A P Baronawski *J. Chem. Phys.* **110** 11206 (1999)
174. R S H Liu, J R Edman *J. Am. Chem. Soc.* **90** 213 (1968)
175. R S H Liu, D M Gale *J. Am. Chem. Soc.* **90** 1897 (1968)
176. V L Ermolaev, E B Sveshnikova *Opt. Spektrosk.* **28** 601 (1970) [a]
177. G D Gillispie, E C Lim *Chem. Phys. Lett.* **63** 355 (1979)
178. R O Campbell, R S H Liu *J. Am. Chem. Soc.* **95** 6560 (1973)
179. R A Keller *Chem. Phys. Lett.* **3** 27 (1969)
180. Sh Kobayashi, K Kikuchi, H Kokubun *Chem. Phys. Lett.* **42** 494 (1976)
181. K Kikuchi, H Fukumura, H Kokubun *Chem. Phys. Lett.* **123** 226 (1986)
182. N A Borisevich, L M Bolot'ko, A V Doronin, A A Sukhodola *Opt. Spektrosk.* **63** 1036 (1987) [a]
183. G A Ketsle, L V Levshin, S N Letuta *Opt. Spektrosk.* **68** 344 (1990) [a]
184. G A Ketsle, L V Levshin, Yu N Lantukh, S N Letuta *Izv. Akad. Nauk SSSR, Ser. Fiz.* **54** 473 (1990)
185. J M Larkin, W R Donaldson, T H Foster, R S Knox *Chem. Phys.* **244** 319 (1999)
186. S Reindl, A Penzkofer *Chem. Phys.* **211** 431 (1996)
187. P C C Lee, M A J Rodgers *Photochem. Photobiol.* **45** 79 (1987)
188. V V Ryl'kov, E A Cheshev *Opt. Spektrosk.* **63** 1030 (1987) [a]
189. Y Yaas, M Klissinger, S Zilberg (Eds) *Conical Intersection in Photochemistry, Spectroscopy and Chemical Dynamics*; *Chem. Phys.* **259** (2 – 3) (Spec. Issue) (2000)

[a] — *Opt. Spectrosc. (Engl. Transl.)*
[b] — *Physics-Uspekhi (Engl. Transl.)*
[c] — *Dokl. Chem. Technol., Dokl. Chem. (Engl. Transl.)*